

Calibration and Comparison of the VISSIM and INTEGRATION Microscopic Traffic Simulation Models

by

Yu Gao

Thesis submitted to the Faculty of the
Virginia Polytechnic Institute and State University
in Partial fulfillment of the requirements for the degree of

Master of Science
in
Civil and Environmental Engineering

Hesham Rakha, Chair
Montasir Abbas, Member
Antonio A. Trani Member

September 05, 2008
Blacksburg, Virginia

Keywords: Car-following Models, Measurements of Effectiveness, VISSIM,
INTEGRATION, Microscopic Traffic Simulation

Copyright© 2008, Yu Gao

Calibration and Comparison of the VISSIM and INTEGRATION Microscopic Traffic Simulation Models

Yu Gao

Abstract

Microscopic traffic simulation software have gained significant popularity and are widely used both in industry and research mainly because of the ability of these tools to reflect the dynamic nature of the transportation system in a stochastic fashion. To better utilize these software, it is necessary to understand the underlying logic and differences between them. A Car-following model is the core of every microscopic traffic simulation software. In the context of this research, the thesis develops procedures for calibrating the steady-state car-following models in a number of well known microscopic traffic simulation software including: CORSIM, AIMSUN, VISSIM, PARAMICS and INTEGRATION and then compares the VISSIM and INTEGRATION software for the modeling of traffic signalized approaches.

The thesis presents two papers. The first paper develops procedures for calibrating the steady-state component of various car-following models using macroscopic loop detector data. The calibration procedures are developed for a number of commercially available microscopic traffic simulation software, including: CORSIM, AIMSUN2, VISSIM, Paramics, and INTEGRATION. The procedures are then applied to a sample dataset for illustration purposes. The paper then compares the various steady-state car-following formulations and concludes that the Gipps and Van Aerde steady-state car-following models provide the highest level of flexibility in capturing different driver and roadway characteristics. However, the Van Aerde model, unlike the Gipps model, is a single-regime model and thus is easier to calibrate given that it does not require the segmentation of data into two regimes. The paper finally proposes that the car-following parameters within traffic simulation software be link-specific as opposed to the current practice of coding network-wide parameters. The use of link-specific parameters will offer the opportunity to capture unique roadway characteristics and reflect roadway capacity differences across different roadways.

Second, the study compares the logic used in both the VISSIM and INTEGRATION software, applies the software to some simple networks to highlight some of the differences/similarities in modeling traffic, and compares the various measures of effectiveness derived from the models. The study demonstrates that both the VISSIM and INTEGRATION software incorporate a psycho-physical car-following model which accounts for vehicle acceleration constraints. The INTEGRATION software, however uses a physical vehicle dynamics model while the VISSIM software requires the user to input a vehicle-specific speed-acceleration kinematics model. The use of a vehicle dynamics model has the advantage of allowing the model to account for the impact of roadway grades, pavement surface type, pavement surface condition, and type of vehicle tires on vehicle acceleration behavior. Both models capture a driver's willingness to run a yellow light if conditions warrant it. The VISSIM software incorporates a statistical stop/go probability model while current development of the INTEGRATION software includes a behavioral model as opposed to a statistical model for modeling driver stop/go decisions. Both

software capture the loss in capacity associated with queue discharge using acceleration constraints. The losses produced by the INTEGRATION model are more consistent with field data (7% reduction in capacity). Both software demonstrate that the capacity loss is recovered as vehicles move downstream of the capacity bottleneck. With regards to fuel consumption and emission estimation the INTEGRATION software, unlike the VISSIM software, incorporates a microscopic model that captures transient vehicle effects on fuel consumption and emission rates.

Acknowledgements

I really don't know how to express my sincere appreciate in one word to the people who helped me in many ways to finish this thesis. But I really would like to thank all of them.

First of all, I want to show my great appreciation to my respected advisor, Dr. Hesham A. Rakha who generously and continuously supports me both academically and financially. He is a patient, knowledgeable, experienced and distinguished professor. It is my luck and great honor to be his student. Although I am still not excellent enough, however, I would say that without his help, I will never be a student like what I am now.

Also, I am very thankful to Dr. Montasir Abbas, who is my committee member and my TA advisor. I really appreciate his priceless advice and recommendations. I would also like to extend my thanks to Dr. Antonio A. Trani and Dr. Mazen Arafeh who provided me with invaluable help.

Finally, I'm truly indebted to my family for their love, support, and encouragement.

Attribution

Professor Hesham Rakha aided in the writing and research behind this thesis. A brief description of his background and his contributions are included here.

Prof. Hesham A. Rakha - Ph.D. (Department of Civil Engineering, Virginia Tech) is my Advisor and Committee Chair. Prof. Rakha provided significant guidance in all chapters of this thesis. Prof. Rakha wrote the first paper “Calibration of Steady-state Car-following Models using Macroscopic Loop Detector Data”. Furthermore, he helped in analyzing the comparison results of VISSIM and INTEGRATION in Chapter 4.

My contribution to Chapter 3 was conducting the research on Wiedemann’s car-following model as well as running the VISSIM software to validate the calibration procedure of the Wiedemann 74 model. For Chapter 4, I conducted research using both the VISSIM and INTEGRATION software, compared the software, and wrote the first draft of the paper.

Table of Contents

Chapter 1: Introduction	1
1.1 Background Information	1
1.2 Problems Definition	1
1.3 Research Objectives and Contributions	1
1.4 Thesis Layout	2
Chapter 2: Literature Review	3
2.1 Introduction of Five Microscopic Traffic Simulation Software	3
2.1.1 AIMSUN	3
2.1.2 VISSIM	3
2.1.3 PARAMICS	4
2.1.4 CORSIM	4
2.1.5 INTEGRATION:	4
2.2 Car-following logic of Five Microscopic Traffic Simulation Software	5
2.2.1 Car-following logic of AIMSUN	5
2.2.2 Car-following logic of VISSIM	6
2.2.3 Car-following logic of PRAMICS	6
2.2.4 Car-following logic of CORSIM	7
2.2.5 Car-following logic of INTEGRATION	7
2.3 Lane-changing logic of Five Microscopic Traffic Simulation Software	8
2.3.1 Lane-changing logic of AIMSUN	8
2.3.2 Lane-changing logic of VISSIM	8
2.3.3 Lane-changing logic of PARAMICS	9
2.3.4 Lane-changing logic of CORSIM	9
2.3.5 Lane-changing logic of INTEGRATION	9
Chapter 3: Calibration of Steady-state Car-following Models using Macroscopic Loop Detector Data	10
3.1 Abstract	10
3.2 Introduction	10
3.3 Traffic Simulation Car-Following Models	11
3.3.1 CORSIM Software	12
Table 2: Steady-State Model Calibration	15
3.3.2 AIMSUN2 Software	16
3.3.3 VISSIM Software	19
3.3.4 Paramics Software	23
3.3.5 INTEGRATION Software	25
3.4 Traffic Stream Model Calibration	27
3.5 Conclusions	29
3.6 Acknowledgement	29
Chapter 4: Comparison of VISSIM and INTEGRATION Software for Modeling a Signalized Approach	30
4.1 Abstract	30
4.2 Introduction	31
4.3 Longitudinal Vehicle Motion Modeling	31
4.3.1 VISSIM Longitudinal Vehicle Motion Modeling	31

4.3.2 INTEGRATION Longitudinal Vehicle Motion Modeling	33
Steady-State Modeling.....	33
Vehicle Deceleration Behavior	34
Vehicle Acceleration Modeling	35
4.4 Modeling Driver and Vehicle Behavior.....	36
4.4.1 Driver Behavior in Response to Yellow Phase Transition	36
4.4.2 Vehicle Modeling.....	37
4.5 Estimation of Measures of Effectiveness.....	38
4.5.1 Estimation of Delay	38
4.5.2 Estimation of Vehicle Stops.....	38
4.5.3 Estimation of Vehicle Fuel Consumption and Emissions.....	39
4.6 Calibration of steady-state Car-following Model	40
4.7 Comparison of VISSIM and INTEGRATION Results	43
4.7.1 Network and Modeling Overview	43
4.7.2 Comparison of Driver Behavior in Response to Traffic Signal Indications	43
4.7.3 The Effects of the “Look-ahead Distance” on VISSIM Driver Behavior	45
4.7.4 Effect of Braking Ability on VISSIM Driver Behavior.....	47
4.7.5 Comparison Driver Behavior Depending on Facility Type.....	47
4.7.6 Comparison of Saturation Flow Rates and Discharge Headways	48
4.7.7 Comparison of Delay Estimates.....	49
4.7.8 Comparison of Fuel Consumption Estimates	50
4.8 Study Conclusions	50
Chapter 5: Conclusions and Recommendations for Future Study	52
5.1 Conclusions.....	52
5.1.1 Calibration and Comparison of Steady-state Car-following Models.....	52
5.1.2 Comparison of VISSIM and INTEGRATION Software.....	52
5.2 Recommendations.....	53
Bibliography	54

List of Figures

Figure 2-1 The different thresholds and regimes in the Fritzsche car-following model.....	6
Figure 2-2: Lane-changing zones of AIMSUN lane-changing model.....	8
Figure 3-1: Example Illustration of Pipes Model Calibration	16
Figure 3-2: Example Illustration of Gipps Model Calibration.....	19
Figure 3-3: Sample Calibration of the Weidemann74 Model.....	21
Figure 3-4: Weidemann74 Calibration Procedure Validation	22
Figure 3-5: Fritzsche’s Car-following Model: a) Thresholds and Regimes, b) and c) Steady-state Behavior.....	23
Figure 3-6: Sample Calibration of the Fritzsche Model	25
Figure 3-7: Sample Calibration of the Van Aerde Model.....	27
Figure 4-1: Illustration of Wiedemann’s Car-following Model	32
Figure 4-2: INTEGRATION Car-following Logic.....	33
Figure 4-3: Wiedemann74 Calibration Procedure Validation.....	42
Figure 4-4: Comparison of Vehicle Speed and Acceleration Profiles (a) Entry 1 s; (b) Entry at 31 s; (c) Entry at 41 s; (d) Entry at 56 s.....	44
Figure 4-5: Comparison of Vehicle Speed and Acceleration Profiles (a) Look-ahead Distance 50 m; (b) Look-ahead Distance of 89 m; (c) Look-ahead Distance of 90 m; (d) Look-ahead Distance of 150 m.....	46
Figure 4-6: Comparison of Vehicle Speed and Acceleration Profiles (a) Look-ahead Distance of 250 m (b) Look-ahead Distance of 700 m.....	47
Figure 4-7: Example of VISSIM Urban and Freeway Speed Profile Comparison.....	48
Figure 4-8: Comparison of Discharge Saturation Flow Rates.....	48
Figure 4-9: Illustration of Discharge Saturation Flow Rates (a) VISSIM and (b) INTEGRATION.....	49
Figure 4-10: Delay Comparison.....	50
Figure 4-11: Fuel Consumption Comparison.....	50

List of Tables

Table 1: Software Car-following Model Formulations	13
Table 2: Steady-State Model Calibration.....	15

Chapter 1: Introduction

1.1 Background Information

The application of microscopic simulation as a tool to reflect real-world traffic systems is increasing in popularity in recent years. The number of traffic simulation models has increased significantly and by the end of the last century, there were more than 70 simulation models available according a study by U.C. Berkley (Skabardonis, 1999). To better utilize these simulation models, there is an obvious need to compare them in detail. Besides, a reliable use of micro-simulation software also requires a rigorous calibration effort. Because traffic simulation software are commonly used to estimate macroscopic traffic stream measures, such as average travel time, roadway capacity, and average speed, the state-of-the-practice is to systematically alter the model input parameters to achieve a reasonable match between desired macroscopic model output and field data.

1.2 Problems Definition

Among the large amount of traffic simulation models, five well-known models are the CORSIM, the AIMSUN2, the VISSIM, the PARAMICS, and the INTEGRATION microscopic traffic simulation models. Each traffic simulation model has its unique underlying logic. This logic includes a car-following logic, a lane-changing logic, and a gap acceptance logic.

“Car-following models form the basis of microscopic simulation models, and they explain the behavior of drivers in a platoon of vehicles.” (Aycin and Benekohal, 1999). Steady-state car-following is extremely critical to traffic stream modeling given that it influences the overall behavior of the traffic stream. Specifically, it determines the desirable speed of vehicles at different levels of congestion, the roadway capacity, and the spatial extent of queues. Comparison of the steady-state car-following models in AIMSUN2, VISSIM, PARAMICS, CORSIM and INTEGRATION and calibration of these steady-state car-following models using field data will help transportation analysts understand how these models work and aid them in future applications.

Although numerous papers have compared different traffic simulation software, it appears that none of these papers have compared the VISSIM and INTEGRATION models in a systematic fashion considering individual driver behavior and vehicle characteristics. Consequently, a detailed comparison between these two models is necessary.

1.3 Research Objectives and Contributions

The objectives of this research effort are two-fold. First, it compares the steady-state car-following models in AIMSUN2, VISSIM, PARAMICS, CORSIM and INTEGRATION and then develops calibration procedures for each of these models using field loop detector data. Second, the research presents a detailed comparison of the VISSIM and INTERATION software for the modeling of signalized approaches.

This thesis makes two significant contributions:

- a. The study develops a systematic calibration procedure for different car-following models that is based on macroscopic traffic stream data

- b. This study provides a systematic comparison of the VISSIM and INTEGRATION software that highlights some of the differences/similarities in modeling traffic, and compares the various measures of effectiveness derived from the models.

1.4 Thesis Layout

This thesis is composed of five chapters. The second chapter provides a detailed review of the five microscopic traffic simulation models AIMSUN2, VISSIM, PARAMICS, CORSIM and INTEGRATION in terms of the car-following and lane-changing logic. The third chapter presents a calibration procedure for the steady-state car-following models of these software applications. The fourth chapter presents a detailed comparison of the VISSIM and INTEGRATION software for modeling a signalized approach. Finally, the fifth chapter concludes with the conclusions of the study and recommendations for future research.

Chapter 2: Literature Review

“The accuracy of a traffic-simulation system depends highly on the quality of the traffic-flow model at its core, with the two main critical components being the car-following and lane-changing models.”(Panwai and Dia, 2005). In this chapter, first, a description of five widely-used microscopic traffic simulation models (AIMSUN2, VISSIM, PARAMICS, CORSIM and INTEGRATION) studied in this thesis is presented. Second, the car-following models of the software are introduced given that in Chapter 3 the research focus is on the steady-state conditions of these car-following models. Third, as lane-changing logic is also a very important logic in simulation models, the lane-changing logic of the five models is discussed.

2.1 Introduction of Five Microscopic Traffic Simulation Software

2.1.1 AIMSUN

AIMSUN, which is short of Advanced Interactive Microscopic Simulator for Urban and Non-Urban Networks, was developed by the Department of Statistics and Operational Research, Universitat Politecnica de Catalunya, Barcelona, Spain.(Xiao et al 2005). This microscopic traffic simulation software is capable of reproducing various real traffic networks and conditions on a computer platform. The driver behavior models inside AIMSUN such as car-following model, lane changing model and gap-acceptance model provide the behavior of each single vehicle of the entire simulation period. (TSS, 2006)

As developed in the GETRAM simulation environment, AIMSUN has the Application Programming Interface (API), which enables it to communicate with some user-defined applications. The advantage of AIMSUN also includes the capability of modeling a traffic network in detail and producing a number of measures of effectiveness. The latest version of AIMSUN at the time of the study was Version 5.1.

2.1.2 VISSIM

VISSIM is a time step and behavior based microscopic traffic simulation model developed at the University of Karlsruhe, Karlsruhe, Germany, in the early 1970s. PTV Transworld AG, a German company, began the commercial distribution of VISSIM from 1993 and continues to maintain the software up to this date. This traffic simulation software is developed to model urban traffic and public transit operations and it is composed of two main components: a traffic simulator and signal state generator. The traffic simulator is in charge of the movement of vehicles, while the signal state generator models the signal status decision from detector information of the traffic simulator and then passes the signal status back to the traffic simulator. (Bloomberg and Dale, 2000)

The VISSIM model can produce almost all the commonly used measurements of effectiveness in the traffic engineering area. Also, it is capable of modeling different vehicle types for both freeways and arterials under different complex traffic control situations. (Moen et al, 2000). The latest version of VISSIM is Version 4.30.

2.1.3 PARAMICS

PARAMICS is a widely used microscopic traffic simulation tool initially developed at the University of Edinburgh in the early 1990's and was introduced commercially in 1997 by SAIS Limited and Quadstone Limited in the UK.

The advantages of PARAMICS include the real-time dynamic three-dimensional visible user interface, which is easy to operate and understand; capable of using a large number of functionalities to simulate a traffic network and to “evaluate various policies and control strategies and their effects on the transportation network such as vehicle delays and emissions”; similar to AIMSUN, the model allows for the overriding or extending the default models using API (Application Programming Interface) (Quadstone, 2003). The latest version of PARAMICS is Version V6.

2.1.4 CORSIM

CORSIM (CORridor SIMulation) is a microscopic simulation model developed by the Federal Highway Administration (FHWA) in 1996. It is one of the most commonly used micro-simulation programs for modeling vehicle traffic operations including the analysis of freeways, urban streets, and corridors or networks.

The model of CORSIM consists of two predecessor models: FRESIM and NETSIM. FRESIM is a freeway model that models uninterrupted facilities including grade separated expressways and interstate freeways; NETSIM is an arterial model that models arterials with at-grade intersections. Both FRESIM and NETSIM have longer history than CORSIM, but the advantage of CORSIM is that it has been applied to many projects (Minnesota Department of Transportation, 2004). The latest version of CORSIM is Version 6.0.

2.1.5 INTEGRATION:

The INTEGRATION 2.30, developed by the late Michel Van Aerde in 1983, is a trip-based microscopic traffic simulation model. Professor Hesham Rakha continues with the development of this model since 1999.

The two most important features of the INTEGRATION software are first, it is the first model to attempt to integrate both freeways and arterials; second, it integrates traffic assignment and microscopic simulation within the same model. The name INTEGRATION stems from this fact. The INTEGRATION model is capable of providing sufficient detailed driver behavior data by tracing individual vehicle movements from its origin to its destination at a level of resolution of one deci-second. Also, the model is capable of computing a number of measurements of effectiveness including vehicle delay, vehicle stops, emissions and fuel consumption as well as the crash risk for 14 crash types. (Van Aerde and Rakha, 2007).

2.2 Car-following logic of Traffic Simulation Software

2.2.1 Car-following logic of AIMSUN

The car following model used in AIMSUN is based on the model developed by Gipps (1981), which considers the speed of the following vehicle to be either free or constrained by the leading vehicle. Below is the detailed description of the model.

The speed of the following vehicle during the time interval $[t, t+T]$ is calculated using equation (1)

$$v_n(t+T) = \min \{v_n^a(t+T), v_n^b(t+T)\} \quad (1)$$

where $v_n^a(t+T)$ is the maximum speed the following vehicle can accelerate and $v_n^b(t+T)$ is the maximum safe speed for the following vehicle with respect to the vehicle in front at time t . Equation (2) is used when the traffic flows freely which means no leading vehicle's impact on its behavior. Equation (3) is used in congested flow conditions which means the behavior of the following vehicle is constrained by the vehicle ahead of it.

$$v_n^a(t+T) = v_n(t) + 2.5 \cdot a_n^{\max} \cdot T \cdot \left(1 - \frac{v_n(t)}{v_n^{\text{desired}}}\right) \cdot \sqrt{0.025 + \frac{v_n(t)}{v_n^{\text{desired}}}} \quad (2)$$

$$v_n^b(t+T) = d_n^{\max} \cdot T + \sqrt{(d_n^{\max} \cdot T)^2 - d_n^{\max} \cdot [2\{x_{n-1}(t) - s_{n-1} - x_n(t)\} - v_n(t) \cdot T - \frac{v_{n-1}(t)^2}{\hat{d}_{n-1}}]} \quad (3)$$

where

a_n^{\max} Maximum desired acceleration, vehicle n , $[m/s^2]$

d_n^{\max} Maximum desired deceleration, vehicle n , $[m/s^2]$

\hat{d}_{n-1} Estimation of maximum deceleration desired by vehicle $n-1$, $[m/s^2]$

T The apparent reaction time, a constant for all vehicles

s_{n-1} The effective length of a vehicle, which consists of vehicles length and the user

specified parameter- min distance between vehicles.

The leader's desired deceleration \hat{d}_{n-1} can be estimated in the following two ways as demonstrated in equation (4) and (5) (TSS, 2002)

$$\hat{d}_{n-1} = d_{n-1} \quad (4)$$

$$\hat{d}_{n-1} = \frac{d_n + d_{n-1}}{2} \quad (5)$$

where the first desired deceleration is calculated to be the estimation as the leaders desired deceleration, d_{n-1} and the second desired deceleration is estimated as average of the leader's and the follower's desired decelerations.

2.2.2 Car-following logic of VISSIM

VISSIM uses a psycho-physical car-following model based on the model developed by Wiedemann (1974), which defines the driver perception thresholds and the regimes formed by these thresholds. There is another car-following model called Wiedemann 99 car-following in VISSIM, the Wiedemann 99 car-following model is in many ways similar to Wiedemann 74 car-following model, except that some of the thresholds in the 99 model are defined in a different (sometimes, simpler) way to model freeway traffic better. In addition, many more of the thresholds are user adjustable in the Wiedemann 99 model. The detailed description of Wiedemann's car-following model is illustrated in Chapter 3.

2.2.3 Car-following logic of PRAMICS

The car following model in PARAMICS, similar with Wiedemann's car-following model, is based on a psycho-physical model developed by Fritzsche (1994). In Fritzsche's model, the perception thresholds and different regimes are defined as demonstrated in figure (2-1). For different regimes the model has its corresponding driver behavior.

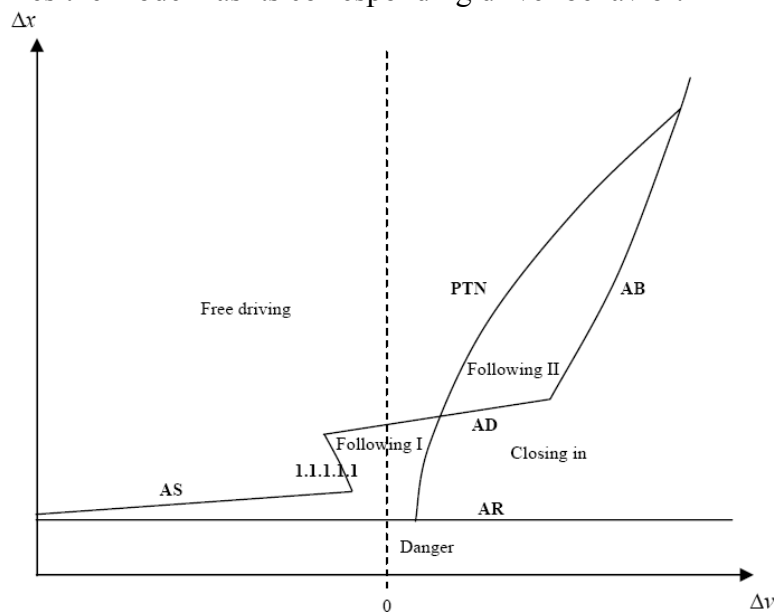


Figure 2-1 The different thresholds and regimes in the Fritzsche car-following model.

In danger regime, the following vehicle uses its max deceleration to extend the headway; in closing in regime, the following need deceleration to keep a distance from the leading vehicle; in following I regime, there is no need for action and as the driver doesn't have the ability to maintain the constant speed, a parameter is assigned to model this; in following II regime, no action is necessary because although the following vehicle realizes he/she is closing in the front vehicle but the distance headway is too large to make any adjustment; in free driving regime, the vehicle accelerates to its desired speed first and then drives around this speed as the driver is unable to maintain the constant speed (Olstam and Tapani, 2004).

2.2.4 Car-following logic of CORSIM

The CORSIM car following model developed by FHWA evolved from two parts: NETSIM and FRESIM models. In which NETSIM models arterials with atgrade intersection and FRESIM models uninterrupted facilities.

FRESIM Car-Following Behavior

FRESIM was developed based on INTRAS, a microscopic freeway simulation application introduced in 1980s. The car-following logic in FRESIM is kept the same as in INTRAS which is Pitt car-following model developed by the University of Pittsburgh (Halati *et al.*, 1996). The basic model of CORSIM takes the distance headway and speed differential between the leading and following vehicle as two independent variables, as shown in Equation(6) (Rakha H. and Crowther B. 2003)

$$h = h_j + c_3 u + b c_3 \Delta u^2 \quad (6)$$

where h and h_j are respectively the distance headway and the jam distance headway(km); u and Δu are respectively the speed of the following vehicle and speed difference between the leading and following vehicles; c_3 is the driver sensitivity factor and b is calibration constant.

NETSIM Car-Following Behavior

The basic logic of NETSIM car-following model is that the following vehicle will move to a certain location where even the leading vehicle decelerates at its maximum deceleration rate, the following vehicle still has enough reaction time and braking ability to stop without resulting in a collision. The basic car-following model is demonstrated in Equation (7) (Rakha H. and Crowther B. 2003). NETSIM utilizes a time step of 1 second in simulation.

$$h = h_j + \Delta s + \Delta r + S_F - S_L \quad (7)$$

Where

Δs = distance traveled by following vehicle over the time interval (km)

Δr = distance traveled by following vehicle during its reaction time (km)

S_F = distance required by following vehicle to come to a complete stop (km)

S_L = distance required by lead vehicle to come to a complete stop (km)

2.2.5 Car-following logic of INTEGRATION

The INTEGRATION software uses the car-following model proposed by Van Aerde (1995) and Van Aerde and Rakha (1995). The Van Aerde's model combines the Greenshields car-following model and the Pipes car-following model into a single-regime model which overcomes the shortcomings of them. "Specifically, the model overcomes the shortcoming of the Pipes model in which it assumes that vehicle speeds are insensitive to traffic density in the uncongested regime." "Alternatively, the model overcomes the main shortcoming of the Greenshields model, which assumes that the speed-flow relationship is parabolic". (Rakha and Crowther, 2002). The detailed description of the car-following in INTEGRATION is presented in Chapter 3.

2.3 Lane-changing Logic Overview

2.3.1 Lane-changing logic of AIMSUN

The lane-changing model applied in AIMSUN is also developed based on the Gipps's lane-changing model (Gipps, 1986). Similar with the other lane-changing models, the lane-changing model in AIMSUN is also a decision based model which addresses three questions: The necessity, desirability and feasibility of the lane change.

The turning feasibility, the distance to next turning and the traffic conditions in the current lane are three dominant factors deciding the necessity of the lane change; the desirability of lane change depends on whether there is improvement after changing lanes, for instance, the speed is faster or the queue length is shorter; the feasibility of lane change means that if there is a sufficient safety distance, lane changing is possible, otherwise it's impossible.

In AIMSUN, three different zones corresponding to different lane changing motivations are considered to generate a more accurate decision, as demonstrated in Figure (2-2). These three zones are defined by the distance to zone 1 and distance to zone 2 in seconds. For zone 1, the main concern about lane change is the traffic condition of these lanes; for zone 2, the desired turning lane is the main concern; for zone 3, the decision of lane changing mainly depends on the feasibility, which means whether the lane change is possible. (Barcelo et al, 2004)

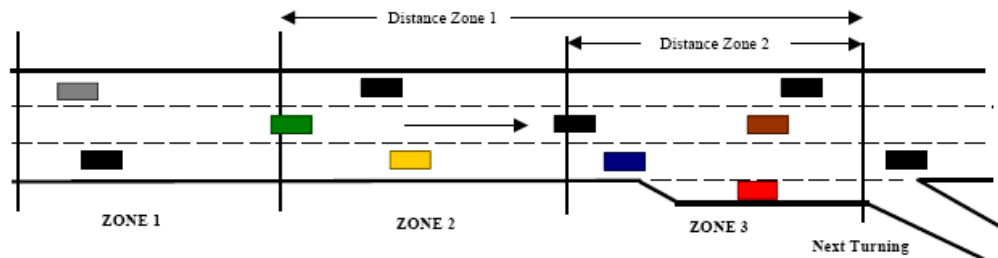


Figure 2-2: Lane-changing zones of AIMSUN lane-changing model

2.3.2 Lane-changing logic of VISSIM

The lane-changing model in VISSIM was originally developed by Willmann and Sparmann (1978). In Sparmann's model, the lane-changing behavior is divided into two types: Lane change to a faster lane and lane change to a slower lane. To make the decision of lane change, three questions need to be evaluated: Whether there is a desire to change the lane, whether the present driving situation in the neighboring lane is favorable, whether the movement to a neighboring lane is possible (Kan and Bhan, 2007). Similar with INTEGRATION, there are also two kinds of lane changes in VISSIM: Necessary lane change and free lane change. The necessary lane change is applied when the vehicle needs to reach the connector of next routine. The free lane change happens when the vehicle is seeking more space or higher speed. No matter which type of lane change it is, the first step for the vehicles in VISSIM is to find "a suitable gap (time headway)" (PTV, 2007)

2.3.3 Lane-changing logic of PARAMICS

Two zones are defined in the PARAMICS lane changing model. For the lane changing zone one, the vehicle has a distance to the junction and the only reason for its lane changes is to overtake a slower vehicle. For the lane changing zone two, the vehicle is approaching the junction and it may choose not to overtake anymore. The lane changes are only for reaching the appropriate lane to make the turn for this zone. (Jiménez et al, 2004)

Duncan (2000) states that the lane changing logic in PARAMICS is applied using “a gap-acceptance policy”. It means that when the vehicle is trying to change to another lane, the following two conditions have to be satisfied: The subject vehicle will not result in a collision with the front vehicle in the target lane; the subject vehicle will not result in a collision with the vehicle behind it in the target lane.

2.3.4 Lane-changing logic of CORSIM

Lane changing logic in CORSIM is based on Gipps’s decision model (1981) which was described earlier. The logic consider mandatory and discretionary lane changes. A mandatory lane change is defined as when the driver must leave the current lane for the next exit. Discretionary lane change is defined as when the driver is seeking better traffic condition in the target lane. The discretionary lane change is not required. (Halati et al, 1997)

2.3.5 Lane-changing logic of INTEGRATION

Both mandatory and discretionary lane changes are considered in INTEGRATION’s lane-changing logic. Mandatory lane change are applied when there is “a need for vehicles to maintain lane connectivity at the end of each link”. In other words, mandatory lane change happens only when the drivers have to shift to another lane in order to leave the road or avoid exiting the road. A discretionary lane change takes place when the drivers are seeking better traffic conditions and the adjacent lane is perceived to provide it.(Rakha and Zhang, 2004).

For discretionary lane changes, first the potential speed at which vehicle could continue to drive in its current lane and the potential speed at which the vehicle could drive after changing to the adjacent left or right lane are computed and compared every deci-second based on the available headway in each lane. The model also scans all lanes on a roadway every 0.5 s. A vehicle might work its way up the lanes to move to a High Occupancy Vehicle (HOV) lane that is empty although all surrounding lanes are less efficient. Second, the vehicle may change to the lane on which it could drive at the highest speed from the previous speed comparison. The precondition of the discretionary lane change is that there must be an adequate gap in the new lane. After the discretionary lane changes are made, the mandatory lane changes become primary in respect of the lane connectivity at the end of the link. The lane changing model in INTEGRATION internally computes the lane connectivity at any diverge or merge, which saves a lot of time for model users of coding link connectivity. (Van Aerde and Rakha, 2007).

Chapter 3: Calibration of Steady-state Car-following Models using Macroscopic Loop Detector Data

Hesham Rakha¹, Yu Gao²

Submitted for publication and presentation at the 88th Transportation Research Board Annual Meeting, Washington DC, January 2009.

3.1 Abstract

The paper develops procedures for calibrating the steady-state component of various car-following models using macroscopic loop detector data. The calibration procedures are developed for a number of commercially available microscopic traffic simulation software, including: CORSIM, AIMSUN2, VISSIM, Paramics, and INTEGRATION. The procedures are then applied to a sample dataset for illustration purposes. The paper then compares the various steady-state car-following formulations and concludes that the Gipps and Van Aerde steady-state car-following models provide the highest level of flexibility in capturing different driver and roadway characteristics. However, the Van Aerde model, unlike the Gipps model, is a single-regime model and thus is easier to calibrate given that it does not require the segmentation of data into two regimes. The paper finally proposes that the car-following parameters within traffic simulation software be link-specific as opposed to the current practice of coding network-wide parameters. The use of link-specific parameters will offer the opportunity to capture unique roadway characteristics and reflect roadway capacity differences across different roadways.

3.2 Introduction

The rapid development of personal computers over the last few decades has provided the necessary computing power for advanced traffic micro-simulators. Today, microscopic traffic simulation software are widely accepted and applied in all branches of transportation engineering as an efficient and cost effective analysis tool. One of the main reasons for this popularity is the ability of microscopic traffic simulation software to reflect the dynamic nature of the transportation system in a stochastic fashion.

The core of microscopic traffic simulation software is a car-following model that characterizes the longitudinal motion of vehicles. The process of car-following consists of two levels, namely modeling steady-state and non-steady-state behavior (Rakha, H. et al, 2004). Ozaki defined steady state as conditions in which the vehicle acceleration and deceleration rate is within a range of $\pm 0.05g$ (Ozaki, 1993). Another definition of steady-state or stationary conditions is provided by Rakha (2006) as the conditions when traffic states remain practically constant over a short time and distance. Steady-state car-following is extremely critical to traffic stream modeling given that it influences the overall behavior of the traffic stream. Specifically, it determines the desirable speed of vehicles at different levels of congestion, the roadway capacity, and the spatial extent of queues. Alternatively, non-steady-state conditions govern the behavior of vehicles while moving from one steady state to another through the use of acceleration and deceleration models. The acceleration model is typically a function of the vehicle dynamics while the deceleration model ensures that vehicles maintain a safe relative distance to the preceding vehicle thus ensuring that the traffic stream is asymptotically stable.

Both acceleration and deceleration models can affect steady-state conditions by reducing queue discharge saturation flow rates.

Traffic stream models describe the motion of a traffic stream by approximating for the flow of a continuous compressible fluid. The traffic stream models relate three traffic stream measures, namely: flow rate (q), density (k), and space-mean-speed (u). Gazis et al. (1961) were the first to derive the bridge between microscopic car-following and macroscopic traffic stream models. Specifically, the flow rate can be expressed as the inverse of the average vehicle time headway. Similarly, the traffic stream density can be approximated for the inverse of the average vehicle spacing for all vehicles within a section of roadway. Therefore every car-following model can be represented by its resulting steady-state traffic stream model. Different graphs relating each pair of the above parameters can be used to show the steady-state properties of a particular model; including the speed-spacing ($u-s$) and speed-flow-density ($u-q-k$) relationships. The latter curve is of more interest, since it is more sensitive to the calibration process and the shape and nose position of the curve determines the behavior of the resulting traffic stream.

A reliable use of micro-simulation software requires a rigorous calibration effort. Because traffic simulation software are commonly used to estimate macroscopic traffic stream measures, such as average travel time, roadway capacity, and average speed, the state-of-the-practice is to systematically alter the model input parameters to achieve a reasonable match between desired macroscopic model output and field data (Dowling.R., et al, 2004). Since the macroscopic flow characteristics are mostly related to steady-state conditions, this requires the user to calibrate the parameters of the steady-state relationship and therefore the knowledge of the steady-state behavior of the car-following model is necessary in this process. It should be mentioned that under certain circumstances, the non-steady-state behavior can also influence steady-state behavior (Rakha, H.A., 2006); however since this is not the general case, the focus of this paper will be on steady-state conditions.

Over the past decade, several car-following models have been proposed and described in the literature. Brackstone and McDonald (1999) categorized the car-following models into five groups, namely: Gazis-Herman-Rothery (GHR) models, safety distance models, linear models, Psycho-physical or action point models, and fuzzy logic based models. However, as it was mentioned above the measures that are usually used by transportation engineers are those of macroscopic nature, which are mostly affected by car-following models. Consequently, calibrating these software using macroscopic data offers a significant appeal to modelers.

The goals of this paper are two-fold. First, the paper identifies the steady-state car-following model for a number of state-of-practice commercial microscopic traffic simulation software. Second, the paper develops a procedure for calibrating these steady-state models using macroscopic loop detector data.

3.3 Traffic Simulation Car-Following Models

The modeling of car-following and traffic stream behavior requires a mathematical representation that captures the most important features of the actual behavior. In this treatment, the relationships obtained by observation, experimentation, and reasoning are given: the

researcher attempts to express their steady-state behavior in a graphical form, and classify them based on their steady-state representation.

Typically, car-following models characterize the behavior of a following vehicle (vehicle n) that follows a lead vehicle (vehicle $n-1$). This can be presented by either characterizing the relationship between a vehicles' desired speed and the vehicle spacing (speed formulation), or alternatively by describing the relationship between the vehicle's acceleration and speed differential between the lead and following vehicles (acceleration formulation).

Over the last few decades, several car-following models have been developed and incorporated within micro-simulation software packages. This section describes the characteristics of six of the state-of-practice and state-of-art car-following models, including the Pitt model (CORSIM), Gipps' model (AIMSUN2), Wiedemann74 and 99 models (VISSIM), Fritzsche's model (PARAMICS), and the Van Aerde model (INTEGRATION). Subsequently, each model is characterized based on its steady-state behavior and procedures are developed to calibrate the model parameters.

It should be noted again that this study only describes car-following behavior under steady-state conditions, when the lead vehicle is traveling at similar speeds and both the lead and following having similar car-following behavior, i.e. $s_n \approx s_{desired}$, $\Delta u_n \approx 0$, where s_n is the spacing between the lead vehicle (vehicle $n-1$) and following vehicle (vehicle n) and Δu_n is the relative speed between the lead and following vehicle ($u_{n-1} - u_n$). In addition to these two conditions, we are capturing the average behavior given that driver behavior is stochastic in nature. The analysis of randomness was presented in an earlier publication (Farzane, M. and H. Rakha, 2006) and thus is not considered further in this research effort.

3.3.1 CORSIM Software

CORSIM was developed by the Federal Highway Administration (FHWA) and combines two traffic simulation models: NETSIM for surface streets and FRESIM for freeway roadways. The FRESIM model utilizes the Pitt car-following model that was developed by the University of Pittsburgh (Halati, A. et al, 1997). The basic model incorporates the vehicle spacing and speed differential between the lead and following vehicle as two independent variables as demonstrated in Table 1 and cast as

$$s_n(t) = s_j + c_3 \frac{u_n(t + \Delta t)}{3.6} + bc_3 \frac{\Delta u_n(t + \Delta t)^2}{3.6^2}, \quad (8)$$

where $s_n(t)$ is the vehicle spacing between the front bumper of the lead vehicle and front bumper of following vehicle at time t (m), s_j is the vehicle spacing when vehicles are completely stopped in a queue (m), c_3 is the driver sensitivity factor (s), b is a calibration constant that equals 0.1 if the speed of the following vehicle exceeds the speed of the lead vehicle, otherwise it is set to zero (h/km), Δu is the difference in speed between lead and following vehicle (km/h) at instant $t+\Delta t$, and u_n is the speed of the following vehicle at instant t (km/h).

Table 1: Software Car-following Model Formulations

Software	Model	Formulation
CORSIM	Pitt Model	$u_n(t + \Delta t) = \min \left(3.6 \cdot \left[\frac{s_n(t) - s_j}{c_3} - b(u_n(t) - u_{n-1}(t))^2 \right], u_f \right)$
VISSIM	Wiedemann 74	$u_n(t + \Delta t) = \min \left\{ \begin{array}{l} 3.6 \cdot \left(\frac{s_n(t) - s_j}{BX} \right)^2 \\ 3.6 \cdot \left(\frac{s_n(t) - s_j}{BX \cdot EX} \right)^2, u_f \end{array} \right\}$
	Wiedemann 99	$u_n(t + \Delta t) = \min \left\{ \begin{array}{l} u_n(t) + 3.6 \cdot \left(CC8 + \frac{CC8 - CC9}{80} u_n(t) \right) \Delta t \\ 3.6 \cdot \frac{s_n(t) - CC0 - L_{n-1}}{u_n(t)}, u_f \end{array} \right\}$
Paramics	Fritzsche	$u_n(t + \Delta t) = \min \left\{ \begin{array}{l} 3.6 \cdot \left(\frac{AD - A_0}{T_D} \right) \\ 3.6 \cdot \left(\frac{AR - A_0}{T_r} \right), u_f \end{array} \right\}$
AIMSUN2	Gipps	$u_n(t + T) = \min \left\{ \begin{array}{l} u_n(t) + 3.6 \left[2.5a_{\max} T \left(1 - \frac{u_n(t)}{u_f} \right) \sqrt{0.025 + \frac{u_n(t)}{u_f}}, \right. \\ \left. 3.6 \left[-bT + \sqrt{b^2 T^2 + b \left(2[s_n(t) - L_{n-1}] - \frac{u_n(t)}{3.6} T + \frac{u_{n-1}(t)^2}{3.6^2 \times b'} \right)} \right] \right\}$
INTEGRATION	Van Aerde	$u_n(t + \Delta t) = \min \left\{ \begin{array}{l} u_n(t) + 3.6 \cdot \frac{F_n(t) - R_n(t)}{m} \Delta t, \\ \frac{-c'_1 + c_3 u_f + \tilde{s}_n(t) - \sqrt{[c'_1 - c_3 u_f - \tilde{s}_n(t)]^2 - 4c_3 [\tilde{s}_n(t) u_f - c'_1 u_f - c_2]}}{2c_3} \end{array} \right\}$ <p>Where: $\tilde{s}_n(t) = s_n(t) + [u_{n-1}(t + \Delta t) - u_n(t)] \Delta t + 0.5a_{n-1}(t + \Delta t) \Delta t^2$</p>

Given that steady-state conditions are characterized by travel at near equal speeds, the third term of the car-following model tends to zero under steady-state driving. Consequently, the steady-state car-following model that is incorporated within FRESIM can be written as

$$s_n(t) = s_j + c_3 \frac{u_n(t + \Delta t)}{3.6} \quad (9)$$

Introducing a constraint on the vehicle speed based on the roadway characteristics and roadway speed limit, the car-following model can be written as

$$u_n(t + \Delta t) = \min \left(u_f, 3.6 \left(\frac{s_n(t) - s_j}{c_3} \right) \right) \quad (10)$$

Rakha and Crowther (2003) demonstrated that the steady-state car-following behavior is identical to the Pipes or the GM-1 model. Furthermore, if we assume that all vehicles are similar in behavior, the vehicle subscripts can be dropped from the formulation. The model then requires the calibration of three parameters, namely: the facility free-flow speed, the facility jam density, and a Driver Sensitivity Factor (DSF) c_3 . In the case of the NETSIM software the parameter is fixed and equal to 1/3600, however in the case of the FRESIM model Rakha and Crowther (2003) showed that the DSF can be related to macroscopic traffic stream parameters as

$$c_3 = 3600 \left(\frac{1}{q_c} - \frac{1}{k_j u_f} \right) \quad (11)$$

where q_c is the mean saturation flow rate (veh/h), k_j is the mean roadway jam density (veh/km), and u_f is the space-mean traffic stream free-flow speed (km/h). For example, considering a freeway facility with an average lane capacity of 2400 veh/h/lane, an average free-flow speed of 100 km/h, and an average jam density of 150 veh/km/lane; the DSF can be computed as 1.26 s, as summarized in Table 2. In other words, the modeler would need to input an average DSF of 1.26 s, a free-flow speed of 100 km/h, and an average vehicle spacing of 6.67 m in order to simulate a saturation flow rate of 2400 veh/h/lane. The estimation of the three macroscopic traffic stream parameters q_c , u_f , and k_j using loop detector data is described later in the paper. Rakha and Crowther (2003) demonstrated the calibration of the DSF can be achieved by changing a base network-wide parameter and changing link-specific adjustment parameters.

The calibration procedure was applied to a sample arterial dataset in which the traffic stream space-mean speed is sensitive to the flow rate in the uncongested regime, as illustrated in Figure 3-1. Because the Pipes model assumes that the traffic stream speed remains constant regardless of the flow rate in the uncongested regime the model is not suitable for such applications. Furthermore, the model assumes that the speed-at-capacity is identical to the free-flow speed, which is not the case in this dataset. It should be noted that the capacity for this example is fairly low given that it is measured upstream of a traffic signal.

Table 2: Steady-State Model Calibration

Car-following Model	Steady-State Calibration
Pitt Model	$c_3 = 3600 \left(\frac{1}{q_c} - \frac{1}{k_j u_f} \right)$
Wiedemann 74	$E(BX) = 1000\sqrt{3.6}\sqrt{u_f} \left(\frac{1}{\alpha q_c} - \frac{1}{k_j u_f} \right) \text{ and } E(EX) = \frac{\frac{k_j u_f}{q_c} - 1}{\frac{k_j u_f}{q_c} - 1 - \alpha q_c} \simeq \alpha$
Wiedemann 99	$CC0 = \frac{1000}{k_j} - \bar{L} \text{ and } CC1 = 3600 \left(\frac{1}{q_c} - \frac{1}{k_j u_f} \right)$
Gipps	<p>b=b': $T = 2400 \left(\frac{1}{q_c} - \frac{1}{k_j u_f} \right)$</p> <p>b>b': Invalid behavior with a non-concave car-following relationship</p> <p>b<b': $b' = \frac{b}{\left(1 - \frac{25920b}{k_j u_c^2} \right)} \text{ and } T = 2.4 \left(\frac{1000}{q_c} - \frac{1000}{k_j u_c} - \frac{u_c}{25.92b} \left(1 - \frac{b}{b'} \right) \right)$</p>
Fritzsche	$A_0 = \frac{1000}{k_j}; T_D = 3600 \left(\frac{1}{q_c} - \frac{1}{k_j u_f} \right); \text{ and } T_r = 3600 \left(\frac{1}{q_c^{\max}} - \frac{1}{k_j u_f} \right)$
Van Aerde	$c_1 = \frac{u_f}{k_j u_c^2} (2u_c - u_f); \quad c_2 = \frac{u_f}{k_j u_c^2} (u_f - u_c)^2; \quad c_3 = \left(\frac{1}{q_c} - \frac{u_f}{k_j u_c^2} \right)$

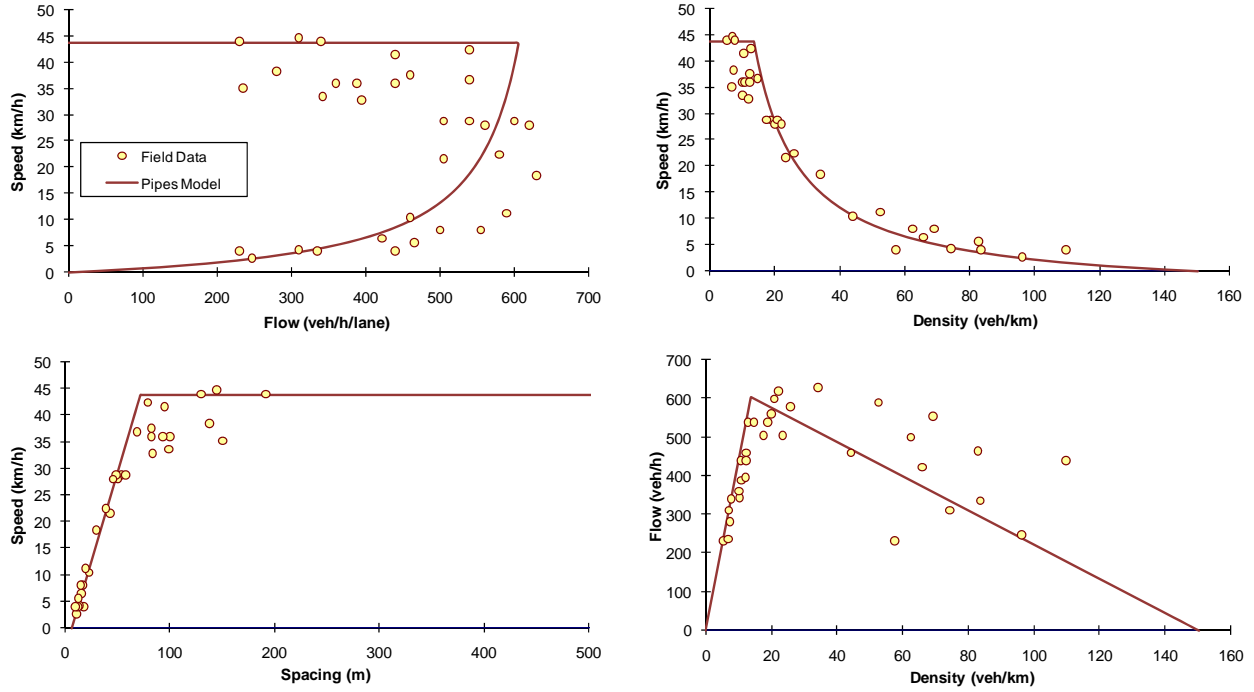


Figure 3-1: Example Illustration of Pipes Model Calibration

3.3.2 AIMSUN2 Software

The AIMSUN2 car-following behavior is modeled using the Gipps car-following model (Gipps, P.G., 1981; Rakha, H. et al, 2007; Wilson, R.E., 2001) and presented in Table 1.

According to Gipps, the speed of the following vehicle is controlled by three conditions. The first condition ensures that the vehicle does not exceed its desired speed or a vehicle-specific free-flow speed (U_n). The second condition ensures that the vehicle accelerates to its desired speed with an acceleration rate that initially increases with speed and then decreases to zero as the vehicle approaches its desired speed. The combination of these conditions results in Equation (12) which controls the vehicle acceleration while vehicles are distant from each other (free-flow behavior). The equation coefficients were obtained from fitting a curve to field data collected on a road of moderate traffic.

$$u_n(t + T) = u_n(t) + 3.6 \left[2.5a_n T \left(1 - \frac{u_n(t)}{U_n}\right) \sqrt{0.025 + \frac{u_n(t)}{U_n}} \right] \quad (12)$$

where $u_n(t)$ is the speed of vehicle n at time t (km/h); a_n is the maximum desired acceleration rate of vehicle n (m/s^2); T is the driver's reaction time (s); and U_n is the desired speed of vehicle n or the vehicle-specific free-flow speed (km/h).

In a constrained traffic situation, when vehicles are traveling close to each other, the third condition becomes dominant and controls the behavior of the follower vehicle while decelerating. The speed of the follower vehicle (see Equation(13)) is affected by the driver reaction time, the spacing between the leader and follower vehicles, the speed of the leader and follower vehicles, and the deceleration rates they are willing to employ. Gipps pointed out that a

safety margin should be added to the driver's reaction time. The safety margin would assure the vehicle's ability to stop even when there is a delay to initiate its reaction for some reason. The safety margin was assumed to be constant in value and equal to $T/2$ (half the reaction time). This safety value is implicit in Equation (13).

$$u_n(t + T) = 3.6 \left[-bT + \sqrt{b^2T^2 + b \left\{ 2[s_n(t) - L_{n-1}] - \frac{u_n(t)}{3.6}T + \frac{u_{n-1}(t)^2}{3.6^2 \times b'} \right\}} \right] \quad (13)$$

Here b and b' are deceleration parameters of vehicle n (m/s^2); b is the actual most severe deceleration rate the vehicle is willing to employ in order to avoid a collision; and b' is the estimated most severe deceleration rate the leader vehicle is willing to employ. It is an estimated value because it is impossible for the follower to evaluate the real intention of his/her leader; L_{n-1} is the effective length of vehicle $n-1$ (the actual length plus a safety margin); $s_n(t)$ is the spacing between vehicle n and $n-1$ at time t (m); and $u_{n-1}(t)$ is the speed of the preceding vehicle (km/h).

The parameters related to deceleration rates (b and b') are very important for the braking process modeling. These parameters influence the spacing between the follower and leader vehicles and thus affect the lane capacity.

Assuming the vehicles will travel as close to their desired speed as possible and considering the dynamics limitations, the speed of vehicle n at time $t + T$ can be computed as

$$u_n(t + T) = \min \left(\begin{array}{l} u_n(t) + 3.6 \left[2.5a_nT \left(1 - \frac{u_n(t)}{U_n} \right) \sqrt{0.025 + \frac{u_n(t)}{U_n}} \right], \\ 3.6 \left[-bT + \sqrt{b^2T^2 + b \left\{ 2[s_n(t) - L_{n-1}] - \frac{u_n(t)}{3.6}T + \frac{u_{n-1}(t)^2}{b'} \right\}} \right] \end{array} \right) \quad (14)$$

According to the above formulation, once the road is unconstrained and the space headways between the vehicles are large enough to allow them to travel at their desired speed, the first argument of Equation (14) is applied. In this case, the following vehicle is able to accelerate according to the empirical equation of vehicle dynamics. Alternatively, in congested conditions, where short headways are typical, the second argument of Equation (14) is applied. In such a case, the speed is limited by the leader vehicle performance. Each vehicle establishes its speed in order to avoid a collision based on the assumption that the leader deceleration rate will not exceed b' .

A detailed mathematical analysis of Gipps' car-following model under steady-state conditions was presented in two earlier publications (Rakha, H. et al, 2007; Wilson, R.E., 2001). Consequently, the paper will only summarize the major findings of these studies and then develop an analytical calibration procedure of the model. In his study, Wilson (2001) presented a mathematical analysis of simplified scenarios and identified parameter regimes that deserve further investigation. The paper also showed the derivation of uniform flow solutions (steady-state) and speed-spacing functions under simplifying conditions concerning parameters b , b' , and T , and an analysis of the linear stability of the uniform flow, identifying stable and non-stable flow regimes. Wilson demonstrated that the steady-state car-following model can be cast as

$$s = s_j + \frac{1}{2.4}Tu + \frac{1}{25.92b}\left(1 - \frac{b}{b'}\right)u^2. \quad (15)$$

Rakha et al. (2007) demonstrated that in the case that b and b' are identical the driver reaction time can be computed as

$$T = 2400\left(\frac{1}{q_c} - \frac{1}{k_j u_f}\right). \quad (16)$$

When b is set greater than b' , Wilson (2001) demonstrated that the car-following relationship may become unphysical and produce multiple solutions for some sets of parameters.

Consequently, b should be set less than or equal to b' . In the case that b is less than b' , Rakha et al. (2007) demonstrated that the steady-state car-following relationship can be cast as

$$u = \min\left(u_f, \left(\frac{5.4bT}{1 - \frac{b}{b'}}\right)\left[-1 + \sqrt{1 + \frac{8000\left(\frac{1}{k} - \frac{1}{k_j}\right)\left(1 - \frac{b}{b'}\right)}{9bT^2}}\right]\right). \quad (17)$$

Starting with Equation (15) the speed-flow relationship can be derived as

$$q = \frac{1000u}{s_j + \frac{1}{2.4}Tu + \frac{1}{25.92b}\left(1 - \frac{b}{b'}\right)u^2}. \quad (18)$$

Using the function of Equation (18) Rakha et al. developed lookup tables to estimate the facility capacity considering different microscopic car-following parameters. This paper extends the research by developing analytical expressions to estimate the microscopic car-following model parameters based on macroscopic traffic stream measurements.

Considering that the maximum flow rate occurs when the first derivative of flow with respect to speed equals to zero, the speed-at-capacity can be computed as

$$u_c = \min\left(3.6 \times \sqrt{\frac{2000b}{k_j\left(1 - \frac{b}{b'}\right)}}, u_f\right). \quad (19)$$

Consequently, we derive the relationship between the microscopic car-following and macroscopic traffic stream parameters as

$$b = \frac{1}{\left(\frac{1}{b'} + \frac{25920}{k_j u_c^2}\right)} \text{ where } b < b', \text{ and} \quad (20)$$

$$T = 2.4\left(\frac{1000}{q_c} - \frac{1000}{k_j u_c} - \frac{u_c}{25.92b}\left(1 - \frac{b}{b'}\right)\right). \quad (21)$$

The calibration of the model entails assuming the most severe deceleration rate the driver is willing to employ (b') and then computing b using Equation (20) for a desired facility-specific mean speed-at-capacity and jam density. The reaction time (T) can then be computed using

Equation (21), as demonstrated in Table 2. It should be noted that in the case that $b=b'$ Equation (21) reverts to Equation (16) given that the speed-at-capacity equals the free-flow speed as computed using Equation (19).

The calibration procedure was applied to the same sample dataset gathered along an arterial, as illustrated in Figure 3-2. The figure demonstrates a reasonable fit to the data, however given that the data demonstrate that traffic stream speed is sensitive to the traffic stream flow in the uncongested regime; the model offers a sub-optimal fit to the field data for the uncongested regime with a good fit for the congested regime. The speed-at-capacity is different from the free-flow speed and thus the model is able to capture this phenomenon.

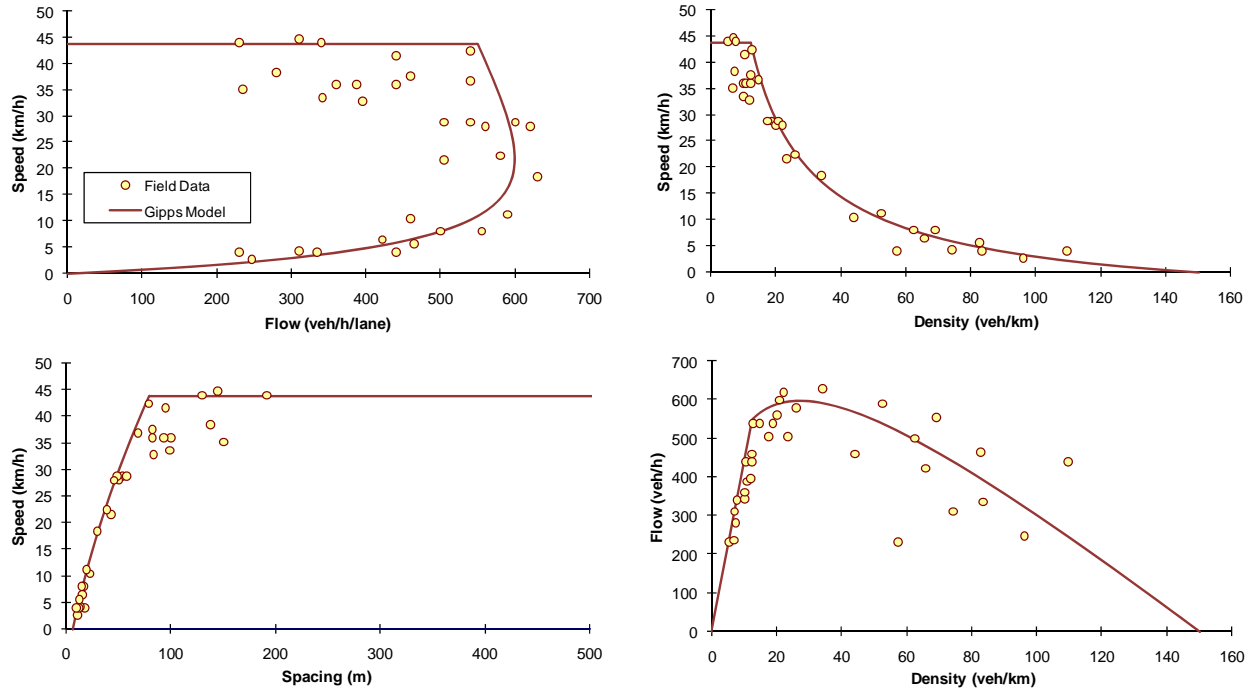


Figure 3-2: Example Illustration of Gipps Model Calibration

3.3.3 VISSIM Software

The car-following model used in VISSIM is a modified version of two models developed by Weidemann (Weidemann74 and 99 models) and belongs to a family of models known as psychophysical or action-point models. This family of models uses thresholds or action-points where the driver changes his/her driving behavior. Drivers react to changes in spacing or relative speed only when these thresholds are crossed. The thresholds and the regimes they define are usually presented in the relative speed/spacing diagram for a pair of lead and follower vehicles.

First the Weidemann74 model is described followed by a description of the Weidemann99 model. For the purposes of this study only the area identified as steady-state is of interest. This area as was mentioned before has the following steady-state criteria ($s_n \approx s_{desired}$, $\Delta u_n \approx 0$). In the case of the Weidemann74 model, the desired vehicle spacing is an interval ($ABX \leq s \leq SDX$) instead of a single value as was the case with previously mentioned models. Given that $\Delta u_n \approx 0$, only the boundaries of desired vehicle spacing interval (ABX & SDX) determine the steady-state characteristics of the VISSIM car-following model. The expected value of ABX and SDX parameters can be calculated as

$$E(AX) = s_j + AX_{add} + AX_{mult} \cdot E(RND1_n) = s_j + 0.5 \approx s_j, \quad (22)$$

$$E(ABX) = E(AX) + E(BX)\sqrt{u} = s_j + E(BX)\sqrt{u}, \quad u \leq u_{desired}, \text{ and} \quad (23)$$

$$E(SDX) = s_j + E(BX) \cdot E(EX)\sqrt{u}, \quad u \leq u_{desired}. \quad (24)$$

Where the BX and EX random variables are computed as

$$BX = BX_{add} + BX_{mult} \cdot RND1_n, \text{ and} \quad (25)$$

$$EX = EX_{add} + BX_{mult} \cdot (NRND - RND2_n). \quad (26)$$

Here $RND1_n$ and $RND2_n$ are user specified vehicle-specific (where n is the vehicle index) normally distributed random variables with a default mean value of 0.5 and a standard deviation of 0.15. $NRND$ is also a normally distributed random variable with a default mean value of 0.5 and standard deviation of 0.15. The expectation of SDX given as $E(SDX)$ ranges between 1.5 to 2.5 times the expected value of ABX ($E(ABX)$), where BX_{add} , BX_{mult} , EX_{add} , and EX_{mult} are user-defined calibration parameters.

Equations (23) and (24) demonstrate that the parameters ABX and SDX are not internally constrained and thus an external maximum speed constraint ($u \leq u_{desired}$) must be enforced. Given that the desired speed is insensitive to traffic conditions ($u_{desired} = u_c = u_f$), the uncongested steady-state behavior has a flat top, as illustrated in Figure 3-3.

In order to calibrate the steady-state Weidemann⁷⁴ model the following calibration procedure is developed. The calibration of the Weidemann⁷⁴ model can be achieved by deriving the speed-flow relationship for the congested regime as

$$q = \frac{1000u}{\frac{1000}{k_j} + \frac{E(BX)E(EX)\sqrt{u}}{\sqrt{3.6}}}. \quad (27)$$

Here u is the traffic stream space-mean speed (km/h); q is the traffic stream flow rate (veh/h), and k_j is the traffic stream density (veh/km). By taking the derivative of flow with respect to speed the relationship is demonstrated to be a strict monotonically increasing function as shown in Equation (28).

$$\frac{dq}{du} = \frac{1000 \left(\frac{1000}{k_j} + \frac{E(BX) \cdot E(EX)\sqrt{u}}{2 \cdot \sqrt{3.6}} \right)}{\left(\frac{1000}{k_j} + \frac{E(BX) \cdot E(EX)\sqrt{u}}{\sqrt{3.6}} \right)^2} > 0 \quad (28)$$

Consequently, the maximum flow occurs at the boundary of the relationship and thus at the maximum desired or free-flow speed. As was the case with the Pipes' model, the speed-at-capacity equals the free-flow speed. By inputting the maximum flow (capacity) and free-flow speed in Equation (27), removing the $E(EX)$ term to compute the capacity upper bound, and rearranging the equation; the expected value of BX can be computed as

$$E(BX) = 1000\sqrt{3.6}\sqrt{u_f} \left(\frac{1}{\alpha q_c} - \frac{1}{k_j u_f} \right). \quad (29)$$

By considering that the expected value of SDX is α times the expected value of ABX (i.e. $E(SDX) = \alpha \times E(ABX)$), where the parameter α ranges from 1.5 to 2.5; the expected value of EX can be computed as

$$E(EX) = \frac{\frac{k_j u_f}{q_c} - 1}{\frac{k_j u_f}{\alpha q_c} - 1} \simeq \alpha \quad (30)$$

Given that $k_j u_f / q_c$ is typically very large, the expected value of EX is approximately equal to the parameter α .

The proposed calibration procedure was applied to the same arterial dataset and the fit is illustrated in Figure 3-3. Again, as was the case with the Pipes' model the fit to the field data is unable to reflect the reduction in traffic stream speed as the arrival rate increases in the uncongested regime. Furthermore, the curvature of the car-following model (speed-spacing diagram) contradicts typical driver behavior (curvature is convex instead of concave). The model does provide a range of behavior for the congested regime as illustrated by the two lines.

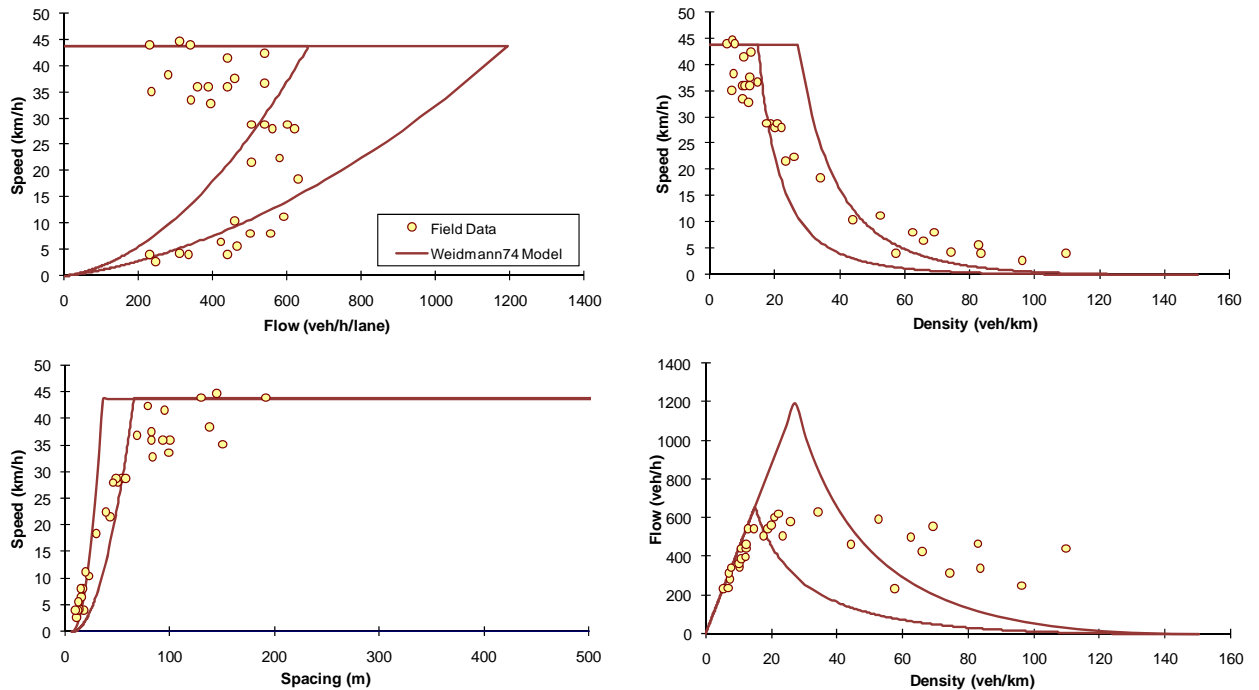


Figure 3-3: Sample Calibration of the Weidemann74 Model

In an attempt to validate the calibration procedure a simple network was coded and simulated using the VISSIM software. The network was composed of two single-lane links in order to isolate the car-following behavior (i.e. remove any possible impact that lane-changing behavior might have on the traffic stream performance). Initially the capacity of both links was set equal using the proposed calibration procedure. The arrival rate was increased gradually until it exceeded the capacity of the entrance link. The traffic stream flow and speed were measured

using a number of loop detectors along the first link. The model randomness was disabled by setting the random variables to zero in order to remove stochastic effects. The results demonstrate that the uncongested regime is flat as was suggested earlier, as illustrated in Figure 3-4. Subsequently, the capacity at the downstream link was reduced by selecting the input parameters using the calibration procedures presented earlier. The demand was fixed at the capacity of the upstream link and thus a bottleneck was created at the entrance to link 2. The departure flow rate and speed were directly measured upstream of the bottleneck to construct the congested regime of the fundamental diagram. As demonstrated in Figure 3-4 the simulated data appear to initially follow the ABX curve and then move towards the SDX curve as the capacity of the downstream bottleneck increases. Given that the movement between the two regimes is not documented in the literature it is not clear how this is done. The figure clearly demonstrates that the proposed calibration procedures are consistent with the VISSIM model output.

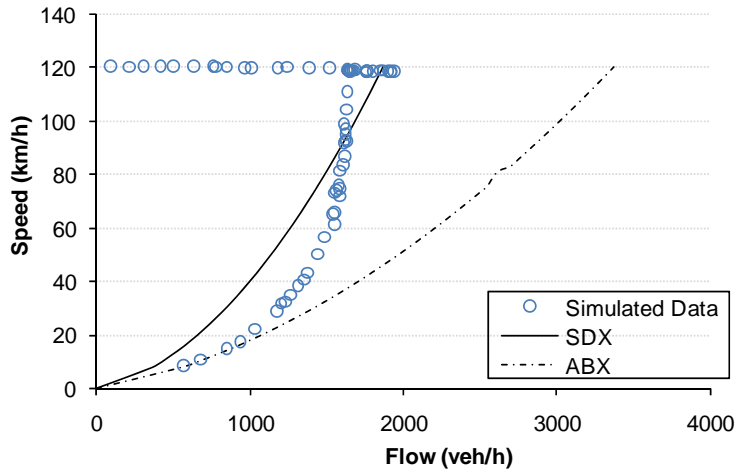


Figure 3-4: Weidemann74 Calibration Procedure Validation

The VISSIM software also offers a second car-following model, namely the Weidemann99 model. The model is formulated as

$$u_n(t + \Delta t) = \min \left\{ \begin{array}{l} u_n(t) + 3.6 \cdot \left(CC8 + \frac{CC8 - CC9}{80} u_n(t) \right) \Delta t \\ 3.6 \cdot \frac{s_n(t) - CC0 - L_{n-1}}{u_n(t)} \end{array} \right\}, u_f \quad (31)$$

This model, as was the case with the Gipps model, computes the vehicle speed as the minimum of two speeds: one based on the vehicle acceleration restrictions and the other based on a steady-state car-following model. The model considers a vehicle kinematics model with a linear speed-acceleration relationship where $CC8$ is the maximum vehicle acceleration at a speed of 0 km/h (m/s^2) and $CC9$ is the maximum vehicle acceleration at a speed of 80 km/h (m/s^2). The VISSIM software also allows the user to input a user-specified vehicle kinematics model that appears to over-ride the linear model. This user specified relationship allows the user to modify the desired and maximum driver speed-acceleration relationship. The second term of Equation (31) computes the vehicle's desired speed using a linear car-following model and thus is identical to the Pipes model.

Consequently, as was done with the Pipes model the model constants $CC0$ and CCI (also known as the Driver Sensitivity Factor) can be computed as

$$CC0 = \frac{1000}{k_j} - \bar{L}, \text{ and} \quad (32)$$

$$CC1 = 3600 \left(\frac{1}{q_c} - \frac{1}{k_j u_f} \right). \quad (33)$$

Where $CC0$ is the spacing between the front bumper of the subject vehicle and the rear bumper of the lead vehicle. This equals the jam density spacing minus the average vehicle length. The Driver Sensitivity Factor (CCI) can be calibrated using three macroscopic traffic stream parameters, namely: the expected roadway capacity, jam density, and free-flow speed.

3.3.4 Paramics Software

The car-following model utilized in the Paramics software, as was the case with the VISSIM software, is a psychophysical car-following model that was developed by Fritzsche (1994). Fritzsche's model uses the same modeling concept as the Weidemann74 car-following model. The difference between these two models is the way thresholds are defined and calculated. Figure 3-5 depicts the Fritzsche model's thresholds in the $\Delta u - \Delta x$ plane.

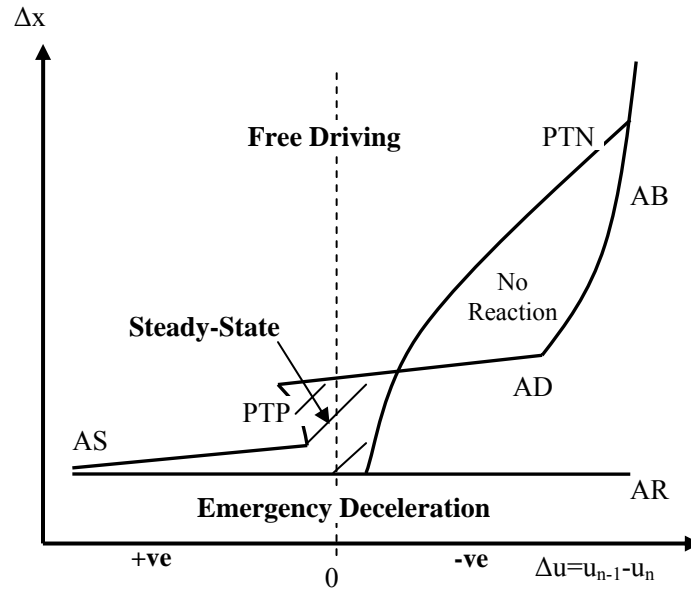


Figure 3-5: Fritzsche's Car-following Model: a) Thresholds and Regimes, b) and c) Steady-state Behavior

The area corresponding to steady-state conditions is almost identical to Weidemann's car-following model. The vehicle spacing for this regime lies between the desired spacing (AD) and the risky spacing (AR). These two boundaries are determined as

$$AR = A_0 + T_r \times \frac{u_n}{3.6}, \text{ and} \quad (34)$$

$$AD = A_0 + T_D \times \frac{u_{n-1}}{3.6}. \quad (35)$$

Where A_0 is the vehicle spacing at jam density, T_r is the risky time gap (usually 0.5 s), T_D is the desired time gap (with a recommended value of 1.8 s). The resulting steady-state car-following model can be written as

$$u_n(t + \Delta t) = \min \left\{ \begin{array}{l} 3.6 \cdot \left(\frac{AD - A_0}{T_D} \right) \\ 3.6 \cdot \left(\frac{AR - A_0}{T_r} \right) \end{array} \right\}, u_f$$

Similar to the Weidemann car-following model, the desired speed constraint must be enforced externally. Again, as was the case with the Weidemann74 model the relationship provides a range of car-following behavior within the congested regime. Unlike the Weidemann74 model the car-following model is linear and thus a Pipes model. Using similar calibration procedures, the various car-following model parameters are related to macroscopic traffic stream parameters as

$$A_0 = \frac{1000}{k_j}; \quad (36)$$

$$T_D = 3600 \left(\frac{1}{q_c} - \frac{1}{k_j u_f} \right); \text{ and} \quad (37)$$

$$T_r = 3600 \left(\frac{1}{q_c^{\max}} - \frac{1}{k_j u_f} \right). \quad (38)$$

The calibration procedure was applied to the same arterial dataset and the results are similar to those of the Weidemann74 model, as illustrated in Figure 3-7. It should be noted that the car-following model provides a range of data in the congested regime considering a linear car-following modeling.

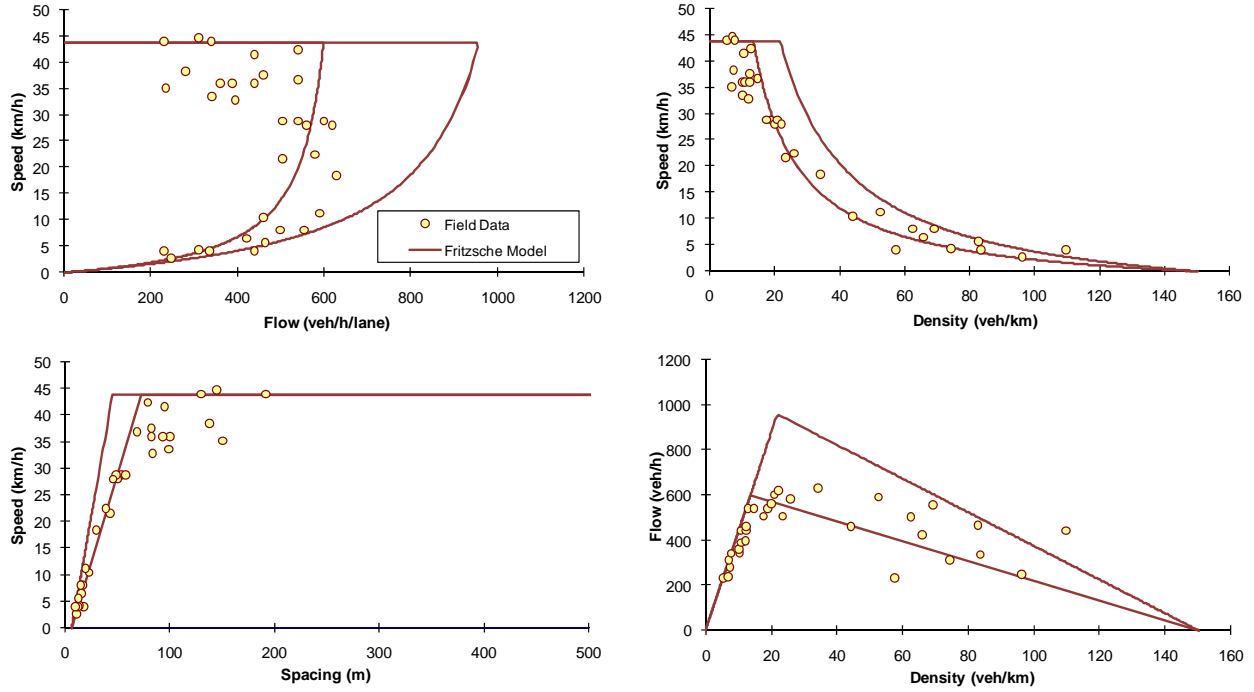


Figure 3-6: Sample Calibration of the Fritzsche Model

3.3.5 INTEGRATION Software

The steady-state functional form that is utilized in the INTEGRATION software is the Van Aerde nonlinear functional form that was proposed by Van Aerde (1995) and Van Aerde and Rakha (1995), which is formulated as

$$s_n(t) = c_1 + c_3 u_n(t + \Delta t) + \frac{c_2}{u_f - u_n(t + \Delta t)}, \quad [39]$$

where c_1 , c_2 , and c_3 are model constants. Demarchi (2002) demonstrated that by considering three boundary conditions the model constants can be computed as

$$c_1 = \frac{u_f}{k_j u_c^2} (2u_c - u_f); \quad c_2 = \frac{u_f}{k_j u_c^2} (u_f - u_c)^2; \quad c_3 = \left(\frac{1}{q_c} - \frac{u_f}{k_j u_c^2} \right). \quad [40]$$

As was demonstrated by Rakha and Crowther (2002) this functional form amalgamates the Greenshields and Pipes car-following models.

Ignoring differences in vehicle behavior within a traffic stream and considering the relationship between traffic stream density and traffic spacing, the speed-density relationship can be derived as

$$k = \frac{1000}{c_1 + \frac{c_2}{u_f - u} + c_3 u}, \quad [41]$$

Of interest is the fact that Equation [41] reverts to Greenshields' linear model, when the speed-at-capacity and density-at-capacity are both set equal to half the free-flow speed and jam density, respectively (i.e. $u_c = u_f/2$ and $k_c = k_j/2$). Alternatively, setting $u_c = u_f$ results in the linear Pipes model given that

$$c_1 = \frac{1}{k_j} = s_j; \quad c_2 = 0; \quad c_3 = \frac{1}{q_c} - \frac{1}{k_j u_f}.$$

Rakha (2006) demonstrated that the wave speed at jam density (denoted as w_j) can be computed by differentiating the speed-density relationship with respect to density at jam density, to be

$$w_j = k_j \left. \frac{du}{dk} \right|_{k_j} = -s_j \left. \frac{du}{ds} \right|_{s_j}. \quad [42]$$

By applying Equation [39] to [41] and ignoring differences between vehicles Rakha derived

$$w_j = -s_j \left. \frac{1}{\frac{ds}{du}} \right|_{u=0} = -\frac{s_j}{c_3 + \frac{c_2}{u_f^2}} = -\frac{u_f}{k_j (c_3 u_f^2 + c_2)} = -\left[\left(\frac{k_j}{q_c} - \frac{u_f}{u_c^2} \right) + \frac{(u_f - u_c)^2}{u_f u_c^2} \right]^{-1}. \quad [43]$$

Considering, a typical lane capacity of 2400 veh/h, a free-flow speed of 110 km/h (which is typical of US highways), and a jam density of 140 veh/km/lane, the wave velocity at jam density ranges between approximately -11.5 to -20.3 km/h, when the speed-at-capacity is varied from 80 to 100% the free-flow speed (which is typical on North American freeways).

As was demonstrated earlier, the Van Aerde model reverts to the Pipes linear model when the speed-at-capacity is set equal to the free-flow speed. Consequently, it can be demonstrated that under this condition the wave speed of [43] reverts to

$$w = -\frac{q_c u_f}{k_j u_f - q_c}, \quad [44]$$

which is the speed of the linear model. Furthermore, when $u_c = u_f/2$ and $k_c = k_j/2$ the wave speed at jam density is consistent with the Greenshields model estimates and is computed as

$$w_j = -u_f. \quad [45]$$

Field observations demonstrate a concave speed-headway relationship. Consequently, the derivative of the speed-density relationship was computed as

$$\frac{du}{ds} = \frac{1}{c_3 + \frac{c_2}{(u_f - u)^2}} = \frac{(u_f - u)^2}{c_3 (u_f - u)^2 + c_2}. \quad [46]$$

Given that the c_2 , c_3 , and u_f parameters are always positive, Rakha (2006) demonstrated the function is a strictly increasing monotonic function. Alternatively, the speed-density relationship is a strictly decreasing monotonic function as

$$\frac{du}{dk} = \frac{du}{ds} \cdot \frac{ds}{dk} = -\frac{(u_f - u)^2}{c_3 (u_f - u)^2 + c_2} \cdot \frac{1}{k^2}. \quad [47]$$

While a strict monotonic function is desired from a theoretical stand point, it is not necessarily reflective of real-life driving behavior. For example drivers might abide by a facility speed limit if they are the only vehicle on a roadway, however if other vehicles are present on the roadway slower drivers might be encouraged to follow faster vehicles recognizing the lower likelihood of

being ticketed for over-speeding. This behavior may only hold when the traffic stream density is very low but contradicts typical traffic flow theory.

The Van Aerde model was calibrated to the same arterial data that were presented earlier, as illustrated in Figure 3-7. The figure demonstrates that the model is extremely flexible and thus is capable of providing a good fit to the field data for the entire range of data both in the uncongested and congested regimes. It should be noted that the fit provides the expected relationship. Differences in driver behavior can be captured by introducing differences in the four traffic stream parameters, namely: free-flow speed, speed-at-capacity, capacity, and jam density.

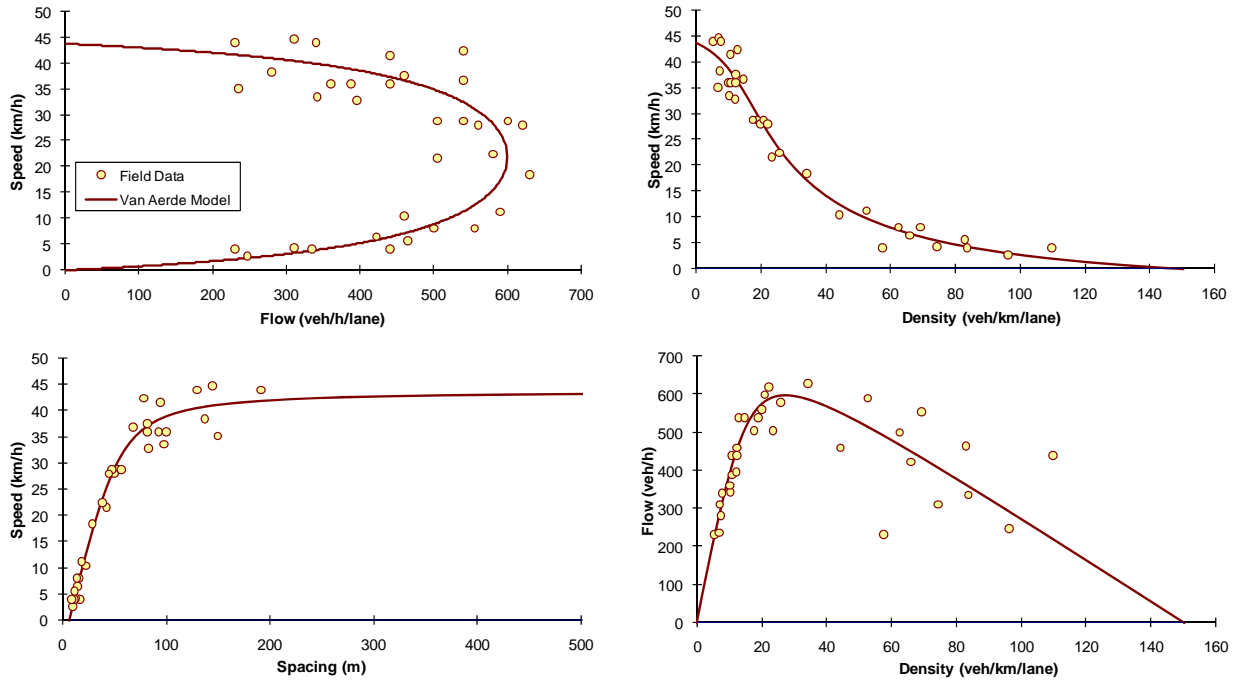


Figure 3-7: Sample Calibration of the Van Aerde Model

3.4 Traffic Stream Model Calibration

The estimation of the four traffic stream parameters (u_f , u_c , q_c , and k_j) requires the calibration of a traffic stream model to loop detector data. This effort entails making four decisions, namely: (1) define the functional form to be calibrated, (2) identify the dependent and the independent variables, (3) define the *optimum* set of parameters, and (4) develop an optimization technique to compute the set of parameter values. Van Aerde and Rakha (1995) and later Rakha and Arafeh (2007) developed a calibration approach that minimizes the orthogonal error about the 3-D fundamental diagram to estimate the expected value of the four traffic stream parameters. The model is briefly described here, however a more detailed description is provided elsewhere (Rakha, H. and M. Arafeh, 2007). The approach is unique because it does not require the identification of dependent and independent variables since it applies a neutral regression approach (minimizes the orthogonal error).

If we consider the Van Aerde functional form given that it provides the highest level of flexibility, as was demonstrated in the previous section, the optimization model can be formulated as

$$\text{Min} \quad E = \sum_i \left\{ \left(\frac{u_i - \hat{u}_i}{\tilde{u}} \right)^2 + \left(\frac{q_i - \hat{q}_i}{\tilde{q}} \right)^2 + \left(\frac{k_i - \hat{k}_i}{\tilde{k}} \right)^2 \right\}. \quad (48)$$

S.T.

$$\begin{aligned} \hat{k}_i &= \frac{1}{c_1 + \frac{c_2}{u_f - \hat{u}_i} + c_3 \hat{u}_i} \quad \forall i \\ \hat{q}_i &= \hat{k}_i \times \hat{u}_i \quad \forall i \\ \hat{q}_i, \hat{k}_i, \hat{u}_i &\geq 0 \quad \forall i \\ \hat{u}_i &< u_f \quad \forall i \\ 0.5u_f &\leq u_c \leq u_f; \quad q_c \leq \frac{k_j u_f u_c}{2u_f - u_c} \\ c_1 &= \frac{u_f}{k_j u_c^2} (2u_c - u_f); \quad c_2 = \frac{u_f}{k_j u_c^2} (u_f - u_c)^2; \quad c_3 = \frac{1}{q_c} - \frac{u_f}{k_j u_c^2} \\ u_f^{\min} &\leq u_f \leq u_f^{\max}; \quad u_c^{\min} \leq u_c \leq u_c^{\max}; \quad q_c^{\min} \leq q_c \leq q_c^{\max}; \quad k_j^{\min} \leq k_j \leq k_j^{\max} \end{aligned} \quad (49)$$

Where u_i , k_i , and q_i are the field observed space-mean speed, density, and flow measurements, respectively. The speed, density, and flow variables with hats (^) are estimated speeds, densities, and flows while the tilde variables (~) are the maximum field observed speed, density, and flow measurements. All other variables are defined as was done earlier in describing the Van Aerde functional form.

The objective function ensures that the formulation minimizes the normalized orthogonal error between the three-dimensional field observations and the functional relationship – in this case the Van Aerde functional form. The three error terms are normalized in order to ensure that the objective function is not biased towards reducing the error in one of the three variables at the expense of the other two variables. This data normalization ensures that the parameters in each of the three axes range from 0.0 to 1.0 and thus a minimization of the orthogonal error provides a quality of fit that is equivalent across all three axes.

The initial set of constraints, which is non-linear, ensures that the Van Aerde functional form is maintained, while the second set of constraints is added to constrain the third dimension, namely the flow rate. The third and fourth set of constraints guarantees that the results of the minimization formulation are feasible. The fifth set of constraints, ensures that the four parameters that are selected do not result in any inflection points in the speed-density relationship (i.e. it ensures that the density at any point is less than or equal to the jam density). A detailed derivation of the final constraint is provided elsewhere (Rakha, H.A., 2006). The sixth set of equations provides estimates for the three model constants based on the roadway's *mean*

free-flow speed (u_f), speed-at-capacity (u_c), capacity (q_c), and jam density (k_j). The final set of constraints provides a valid search window for the four traffic stream parameters that are being optimized (u_f , u_c , q_c , and k_j).

The total number of independent decision variables equals twofold the number of field observations plus the four traffic stream parameters u_f , u_c , q_c , and k_j . For example a problem with 100 observations results in a total of 204 independent decision variables ($2 \times 100 + 4$). The heuristic approach that was developed earlier was applied to the data to estimate the four traffic stream parameters (Van Aerde, M. and H. Rakha, 1995; Rakha, H. and M. Arafteh., 2007). Once the four traffic stream parameters are estimated the individual car-following models can be calibrated using the equations provided in Table 2.

3.5 Conclusions

The paper developed procedures for calibrating the steady-state component of various car-following models using macroscopic loop detector data. The paper then compared the various steady-state car-following formulations and demonstrated that the Gipps and Van Aerde steady-state car-following models provide the highest level of flexibility in capturing different driver and roadway characteristics. However, the Van Aerde model, unlike the Gipps model, is a single-regime model and thus is easier to calibrate given that it does not require the segmentation of data into two regimes. An analysis of existing software demonstrated that a number of car-following parameters are network- and not link-specific and thus do not offer model users with the flexibility of coding different roadway capacities for different facility types. In some software, however, arterial and freeway roadway car-following parameters can be coded separately, as in the case of CORSIM and VISSIM. However, major roadway capacity differences can be observed within the broad range of facility categories. For example the saturation flow rate may vary from 1300 to 2000 veh/h on an arterial depending on the roadway and driver characteristics. Consequently, the paper recommends that modifications be made to the various software to allow more flexibility in setting link-specific car-following parameters.

3.6 Acknowledgement

The authors acknowledge the valuable input from Dr. William Perez of Cambridge Systematics, Inc. and Roemer Alfelor and David Yang of the Federal Highway Administration. Finally, the authors acknowledge the financial support provided by the FHWA and the Mid-Atlantic University Transportation Center (MAUTC) in conducting this research effort.

Chapter 4: Comparison of VISSIM and INTEGRATION Software for Modeling a Signalized Approach

Yu Gao¹, Hesham Rakha²

Submitted for publication and presentation at the 88th Transportation Research Board Annual Meeting, Washington DC, January 2009.

4.1 Abstract

The paper compares the VISSIM and INTEGRATION software for the modeling of traffic signal networks. The software are compared in terms of the modeling of longitudinal vehicle motion, driver behavior within the traffic signal dilemma zone, vehicle acceleration constraints, vehicle discharge headways, and various measures of effectiveness (delay, stops, and fuel consumption). Both software incorporate a psycho-physical car-following model which accounts for vehicle acceleration constraints. The INTEGRATION software, however uses a physical vehicle dynamics model while the VISSIM software requires the user to input a vehicle-specific speed-acceleration kinematics model. The use of a vehicle dynamics model has the advantage of allowing the model to account for the impact of roadway grades, pavement surface type, pavement surface condition, and type of vehicle tires on vehicle acceleration behavior. Both models capture a driver's willingness to run a yellow light if conditions warrant it. The VISSIM software incorporates a statistical stop/go probability model while current development of the INTEGRATION software includes a behavioral model as opposed to a statistical model for modeling driver stop/go decisions. Both software capture the loss in capacity associated with queue discharge using acceleration constraints. The losses produced by the INTEGRATION model are more consistent with field data (7% reduction in capacity). Both software demonstrate that the capacity loss is recovered as vehicles move downstream of the capacity bottleneck. With regards to vehicle fuel consumption and emission estimation the INTEGRATION software, unlike the VISSIM software, incorporates a microscopic model that captures transient vehicle effects on fuel consumption and emission rates.

4.2 Introduction

Although numerous papers have compared different traffic simulation software, however only a few have compared the VISSIM and INTEGRATION software. Furthermore, none of these papers have compared these models in a systematic fashion considering individual driver behavior and vehicle characteristics. For example, an earlier study compared two macroscopic models: *FREQ* and *KRONOS* with two microscopic models: *VISSIM* and *INTEGRATION* (Prevedouros, P.D., W. James, and J. Jerry, 2006) on a 15-mile section of H1 in Honolulu, Hawaii. The study concluded that the calibration of microscopic traffic simulation software is time-consuming and that the results of the models are not necessarily consistent.

This study compares the logic used in both the *VISSIM* and *INTEGRATION* software, applies the software to some simple networks to highlight some of the differences/similarities in modeling traffic, and compare the various measures of effectiveness derived from the models.

Initially, the paper provides an overview of the modeling of longitudinal vehicle motion followed by an overview of the driver and vehicle modeling logic. Subsequently, a comparison of various measures of effectiveness computation is presented followed by some model applications to a sample single signal network. The differences and similarities in the model results are highlighted followed by a summary of the study conclusions.

4.3 Longitudinal Vehicle Motion Modeling

4.3.1 VISSIM Longitudinal Vehicle Motion Modeling

The car-following model in *VISSIM* is a psycho-physical driver behavior model developed by Wiedemann (1974) that defines a driver perception threshold. The different thresholds and regimes in Wiedemann's car-following model are demonstrated in Figure 3-1.

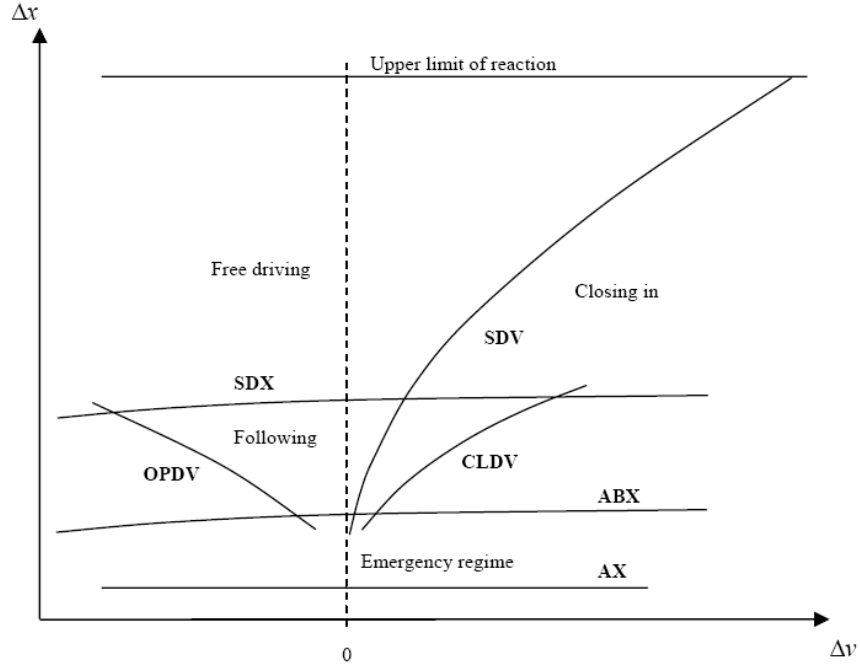


Figure 4-1: Illustration of Wiedemann's Car-following Model

Here the variable AX is the desired following distance between stationary vehicles, ABX is the desired minimum following distance at low speed differences, and SDX is the maximum following distance. These variables are computed using the following equations (Wiedemann, R., 1974).

$$AX = s_j = L_{n-1} + AXadd + RND1_n \cdot AXmult \quad (50)$$

$$ABX = s = s_j + (BXadd + BXmult \cdot RND1_n) \cdot \sqrt{u} \quad (51)$$

$$SDX = s_j + (EXadd + EXmult \cdot (NRND - RND2_n)) \cdot BX \cdot \sqrt{u} \quad (52)$$

Where $AXadd$, $AXmult$, $BXadd$, $BXmult$, $EXadd$, and $EXmult$ are calibrated parameters. $RND1_n$ and $RND2_n$ are normally distributed, driver-dependent parameters, and $NRND$ is a normally distributed random number. From Equations (50) through (52) and the basic traffic stream model $q = ku$, the macroscopic flow-speed relationship can be derived cast as

$$q = \begin{cases} \frac{1000u}{\frac{1000}{k_j} + \frac{BX}{\sqrt{3.6}} \sqrt{u}} \\ \frac{1000u}{\frac{1000}{k_j} + \frac{BX \cdot EX}{\sqrt{3.6}} \sqrt{u}} \end{cases} \quad (53)$$

The first q - u relationship is derived when the vehicle spacing is ABX ; the second q - u relationship is derived when the vehicle spacing is SDX . To help explain Wiedemann's psycho-physical car-following model, the definition of each regime and the corresponding driver behavior, as derived by Olstam and Tapini (2004).

4.3.2 INTEGRATION Longitudinal Vehicle Motion Modeling

The INTEGRATION car-following model falls within the psycho-physical model formulations because it considers a driver within different regimes, as illustrated in Figure 4-2. Specifically, the vehicle will collide with a vehicle if its spacing from the lead vehicle is less than a safe distance that increases as the speed difference between the lead and following vehicle increases (negative speed differential). The driver typically attempts to converge to the steady-state behavior by either decelerating (collision avoidance) or accelerating. The driver is in free-flow mode once the spacing between the following and lead vehicle exceeds a threshold.

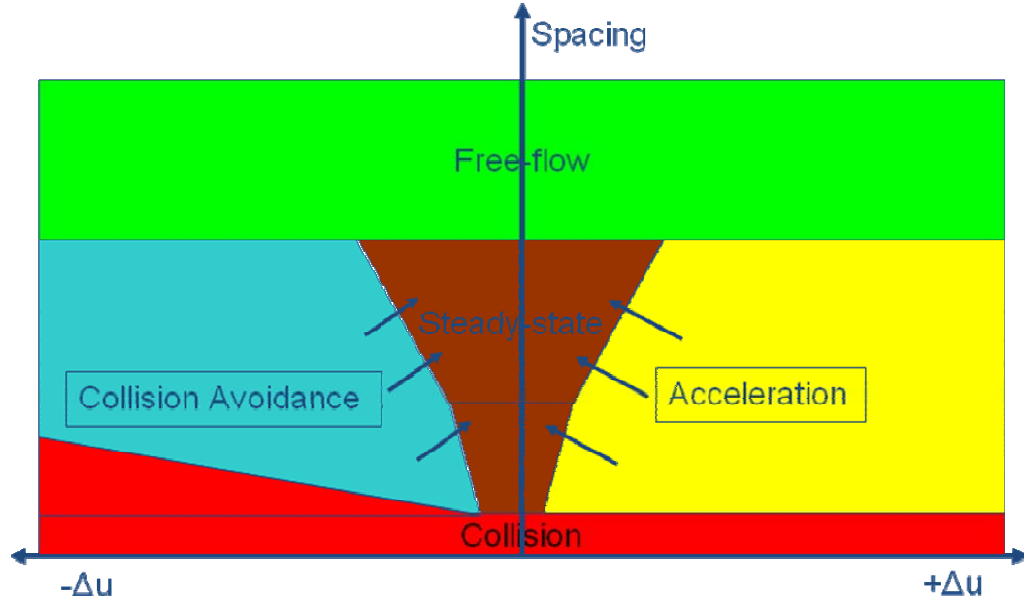


Figure 4-2: INTEGRATION Car-following Logic

The model computes the vehicle speed as the minimum of two speeds, namely: the maximum vehicle speed based on vehicle dynamics and the desired speed based on the Van Aerde car-following model formulation as

$$u_n(t + \Delta t) = \min \left\{ \begin{array}{l} u_n(t) + 3.6 \cdot \frac{F_n(t) - R_n(t)}{m} \Delta t, \\ \frac{-c_1' + c_3 u_f + \tilde{s}_n(t) - \sqrt{[c_1' - c_3 u_f - \tilde{s}_n(t)]^2 - 4c_3 [\tilde{s}_n(t)u_f - c_1' u_f - c_2]}}{2c_3} \end{array} \right\}. \quad (54)$$

Steady-State Modeling

The Van Aerde nonlinear functional form that was proposed by Van Aerde (1995) and Van Aerde and Rakha (1995), is formulated as

$$s_n(t) = c_1 + c_3 u_n(t + \Delta t) + \frac{c_2}{u_f - u_n(t + \Delta t)}, \quad (55)$$

where c_1 , c_2 , and c_3 are model constants. Demarchi (2002) demonstrated that by considering three boundary conditions the model constants can be computed as

$$c_1 = \frac{u_f}{k_j u_c^2} (2u_c - u_f); \quad c_2 = \frac{u_f}{k_j u_c^2} (u_f - u_c)^2; \quad c_3 = \left(\frac{1}{q_c} - \frac{u_f}{k_j u_c^2} \right). \quad (56)$$

As was demonstrated by Rakha and Crowther (2002) this functional form amalgamates the Greenshields and Pipes car-following models.

Ignoring differences in vehicle behavior within a traffic stream and considering the relationship between traffic stream density and traffic spacing, the speed-density relationship can be derived as

$$k = \frac{1000}{c_1 + \frac{c_2}{u_f - u} + c_3 u}, \quad (57)$$

Of interest is the fact that Equation [41] reverts to Greenshields' linear model, when the speed-at-capacity and density-at-capacity are both set equal to half the free-flow speed and jam density, respectively (i.e. $u_c = u_f/2$ and $k_c = k_j/2$). Alternatively, setting $u_c = u_f$ results in the linear Pipes model given that

$$c_1 = \frac{1}{k_j} = s_j; \quad c_2 = 0; \quad c_3 = \frac{1}{q_c} - \frac{1}{k_j u_f}.$$

Rakha (2006) demonstrated that the wave speed at jam density (denoted as w_j) can be computed as

$$w_j = -s_j \frac{1}{\left. \frac{ds}{du} \right|_{u=0}} = -\frac{s_j}{c_3 + \frac{c_2}{u_f^2}} = -\frac{u_f}{k_j (c_3 u_f^2 + c_2)} = -\left[\left(\frac{k_j}{q_c} - \frac{u_f}{u_c^2} \right) + \frac{(u_f - u_c)^2}{u_f u_c^2} \right]^{-1}. \quad (58)$$

Vehicle Deceleration Behavior

The literature (Mannering, F.L. and W.P. Kilareski, 1998) indicates that the maximum braking force acting on each axle can be computed as the coefficient of roadway adhesion multiplied by the vehicle weight normal to the roadway surface. Because true optimal brake force proportioning is seldom achieved in standard non-antilock braking systems, a braking efficiency term is also used in computing the maximum braking force as

$$d_{max} = \eta_b \mu g. \quad (59)$$

Here η_b is the braking efficiency, μ is the coefficient of roadway adhesion also known as the coefficient of friction, and g is the gravitational acceleration (9.8066 m/s²). In the case of antilock braking systems the braking efficiency approaches 100%. Noteworthy is the fact that Equation (59) demonstrates that the maximum vehicle deceleration varies as a function of the roadway conditions as reflected by the coefficient of road friction.

The INTEGRATION model ensures that a vehicle maintains an additional distance to the lead vehicle to allow the following vehicle to decelerate to the speed of the lead vehicle in the event that the following vehicle is closing on the lead vehicle.

Vehicle Acceleration Modeling

Vehicle acceleration is governed by vehicle dynamics. Vehicle dynamics models compute the maximum vehicle acceleration levels from the resultant force acting on a vehicle, as

$$a = f_p \frac{F - R}{m} \quad (60)$$

where a is the vehicle acceleration (m/s^2), F is the vehicle tractive force (N), R is the total resistance force (N), m is the vehicle mass (kg), and f_p is the proportion of the maximum acceleration that the driver is willing to employ (field studies have shown that it is typically 0.62).

The vehicle tractive effort is computed as

$$F_T = 3600 \beta \eta \frac{P}{u} \quad (61)$$

Here F_T is the engine tractive force (N), β is a gear reduction factor that will be described later (unitless), η is the driveline efficiency (unitless), P is the vehicle power (kW), and u is the vehicle speed (km/h).

Given that the tractive effort tends to infinity as the vehicle speed tends to zero, the tractive force cannot exceed the maximum force that can be sustained between the vehicle's tractive axle tires and the roadway surface, which is computed as

$$F_{max} = m_{ta} g \mu \quad (62)$$

Here m_{ta} is the mass of the vehicle on the tractive axle (kg), g is the gravitational acceleration (9.8066 m/s^2), and μ is the coefficient of road adhesion or the coefficient of friction (unitless).

Typical axle mass distributions for different truck types were presented in an earlier publication and thus are not discussed further (Rakha, H., et al., 2001). The tractive force is then computed as the minimum of the two forces as

$$F = \min(F_T, F_{max}) \quad (63)$$

Rakha and Lucic (2002) introduced the β factor into Equation (61), in order to account for the gear shift impacts at low traveling speeds when trucks are accelerating. Specifically, the factor is a linear function of vehicle speed with an intercept of $1/u_0$ and a maximum value of 1.0 at u_0 (optimum speed or the speed at which the vehicle attains its full power) as

$$\beta = \frac{1}{u_0} \left[1 + \min(u, u_0) \left(1 - \frac{1}{u_0} \right) \right] \quad (64)$$

The optimum speed was found to vary as a function of the weight-to-power ratio (for weight-to-power ratios (w) ranging from 30 to 170 kg/kW) as

$$u_0 = 1164w^{-0.75} \quad (65)$$

Here w is the weight-to-power ratio in kg/kW. Rakha and Snare (2004) demonstrated that the gear shift parameter β is not required for the modeling of light-duty vehicle acceleration behavior (weight-to-power is less than 30 kg/kW).

Three resistance forces are considered in the model, namely the aerodynamic, rolling, and grade resistance forces (Mannering, F.L. and W.P. Kilareski, 1998; Rakha, H., et al., 2001). The first resistance force is the aerodynamic resistance that varies as a function of the square of the air speed. Although a precise description of the various forces would involve the use of vectors, for most transportation applications scalar equations suffice if the forces are considered to only apply in the roadway longitudinal direction. For the motion of a vehicle in still air, the air speed equals the vehicles speed as

$$R_a = \frac{\rho}{2 \times 3.6^2} C_d C_h A u^2 = c_1 C_d C_h A u^2, \quad (66)$$

where ρ is the density of air at sea level and a temperature of 15°C (59°F) (equal to 1.2256 kg/m³), C_d is the drag coefficient (unitless), C_h is a correction factor for altitude (unitless), and A is the vehicle frontal area (m²). Given that the air density varies as a function of altitude, the C_h factor can be computed as

$$C_h = 1 - 8.5 \times 10^{-5} H. \quad (67)$$

Typical values of vehicle frontal areas for different vehicle types and typical drag coefficients are provided in the literature (Rakha, H., et al., 2001).

The second resistance force is the rolling resistance, which is a linear function of the vehicle speed and mass, as

$$R_r = C_r (c_2 u + c_3) \frac{mg}{1000}. \quad (68)$$

Typical values for the rolling coefficients (C_r , c_1 , and c_2), as a function of the road surface type, condition, and vehicle tires, are provided in the literature (Rakha, H., et al., 2001). Generally, radial tires provide a resistance that is 25 percent less than that for bias ply tires.

The third and final resistance force is the grade resistance, which accounts for the proportion of the vehicle weight that resists the movement as a function of the roadway grade (i) as

$$R_g = mgi. \quad (69)$$

Having computed the various resistance forces, the total resistance force is computed as

$$R = R_a + R_r + R_g. \quad (70)$$

4.4 Modeling Driver and Vehicle Behavior

4.4.1 Driver Behavior in Response to Yellow Phase Transition

According to the VISSIM manual (PTV, 2007), a vehicle will normally slow down in front of a red traffic signal. At an amber signal, two decision models can be selected to model the vehicle's reaction: a continuous check model and a one-decision model, in which the continuous check model is the default option.

During the simulation, each vehicle's position, speed, and acceleration are computed at each time step (up to 10 time steps per simulation second, called simulation resolution). In the continuous check model, vehicle interaction and decisions are updated at each time

step to model a vehicle approaching an amber signal. With the continuous check, vehicles will proceed through the intersection if they cannot come to a safe stop in front of the stop line. In other words, if vehicles can make a safe stop, they will. In the one-decision model, the decision to continue through an amber indication is based on a calculated probability. Depending on the decision (calculated probability), vehicles may run through the amber even if they could stop within a safe distance, or vehicles may stop even if they could continue safely.

In the current version of the INTEGRATION software, when a vehicle faces a red light, it treats the signal as a stationary vehicle and slows down accordingly. However, when a vehicle faces an amber signal, it has full knowledge of the remaining amber time and makes a decision to run if the time required to run at its current speed is less than the remaining amber time. Otherwise the vehicle elects to stop. This decision is made each deci-second as the vehicle approaches the traffic signal.

Further enhancements to the model will include introducing an error in the driver's estimate of the amber duration. The introduction of such an error will result in vehicles stopping although they could have run the amber, however, because they under-estimate the duration of the amber they elect to stop. Alternatively, drivers might run a red light if they over-estimate the duration of the amber. The error function will be calibrated to replicate field observed driver stop/run probabilities as a function of their time to intersection at the time an amber indication is introduced.

4.4.2 Vehicle Modeling

In the case of the VISSIM software, several vehicle characteristics are assigned prior to executing the software, including the maximum acceleration/deceleration level, speed, weight, and power. To represent different driver behavior for each vehicle type, VISSIM uses acceleration/deceleration functions, rather than single values, to model different levels of maximum acceleration/deceleration and desired acceleration/deceleration levels. These functions decrease as a function of the vehicle speed.

In a similar way, the vehicle's desired speed in VISSIM is also not a single value. Rather, it is assigned in a stochastic distribution with a maximum and minimum value.

Weight and power are two important parameters that have a significant influence on vehicle dynamics as was demonstrated earlier in Equation (60). According to the VISSIM user's manual (5), the software also uses distributions of weight and power, which are applied only to vehicles categorized as HGV. VISSIM randomly selects power and weight values from the distributions and then calculates the power-to-weight ratio. Based on the power-to-weight ratio, an acceleration/deceleration rate is selected from the acceleration/deceleration distributions. The details of this procedure are not provided in the manual.

In INTEGRATION, the vehicle's characteristic parameters can be defined in the vehicle characteristics file. For each vehicle type, vehicle parameters related to the vehicle's dynamic model — including vehicle weight, vehicle power, transmission efficiency, drag

coefficient, etc. — are defined. The detail of the vehicle dynamics model was described earlier in the paper and thus is not described further.

4.5 Estimation of Measures of Effectiveness

This section describes the specifics on how various measures of effectiveness are computed in the VISSIM and INTEGRATION software. Initially, the estimation of vehicle delay is described followed by a description of the procedures for estimating vehicle fuel consumption and emissions.

4.5.1 Estimation of Delay

As demonstrated in Equation (71), the vehicle delay within the INTEGRATION software is estimated as “the difference in travel time between travel at the vehicle’s instantaneous speed and travel at free-flow speed” (Van Aerde, M. and H. Rakha, 2007) as

$$D = \sum_{i=1}^N d_i = \sum_{i=1}^N \left(1 - \frac{u(t+i\Delta t)}{u_f} \right) \cdot \Delta t \quad (71)$$

Where D is the total delay incurred over entire trip; d_i is the delay incurred during interval i ; Δt is the duration of interval; $u(t+i\Delta t)$ is the vehicle instantaneous speed in interval i ; u_f is the expected free-flow speed of the facility on which the vehicle is traveling; and N is the number of time intervals in a speed profile. This model has been validated against state-of-the-art delay estimation procedures using queuing theory and shockwave analysis (Dion, F., H. Rakha, and Y.-S. Kang, 2004). The total delay is then computed as the summation of all instantaneous delays along a link, for an entire trip, and for an entire network. These delay estimates can be segregated across five different vehicle classes.

In the case of the VISSIM software, the vehicle’s delay estimates can be obtained from the vehicle record section, in which delay is defined as “the difference from optimal driving time” (5) in seconds and is estimated every deci-second, as was described in the INTEGRATION software.

4.5.2 Estimation of Vehicle Stops

The VISSIM computes a vehicle stop when a vehicle changes its speed from any speed greater than 0 to a speed of 0, i.e. it is when a vehicle comes to a standstill. The approach does not account for partial stops.

In the case of the INTEGRATION software, each time a vehicle decelerates the drop in speed is recorded as a partial stop, as demonstrated in Equation (72) (Van Aerde, M. and H. Rakha, 2007; Rakha, H., Y.-S. Kang, and F. Dion, 2001). The sum of these partial stops is also recorded. This sum, in turn, provides a very accurate explicit estimate of the total number of stops that were encountered along that particular link.

It is noteworthy that INTEGRATION will often report that a vehicle has experienced more than one complete stop along a link. Multiple stops arise from the fact that a vehicle may have to stop several times before ultimately clearing the link stop line. This finding, while seldom recorded by or even permitted within macroscopic models, is a common

observation within actual field data for links on which considerable over-saturation queues exist. The details of estimating vehicle stops and the validation of the procedure are presented in Volume III of the manual.

$$S = \sum_{i=\Delta t}^T S(t_i) = \sum_{i=\Delta t}^T \frac{u(t_i) - u(t_{i-\Delta t})}{u_f} \quad \forall i \quad \ni u(t_i) < u(t_{i-\Delta t}) \quad (72)$$

4.5.3 Estimation of Vehicle Fuel Consumption and Emissions

In VISSIM, the fuel consumption of an individual vehicle can be obtained from the vehicle record, in which two types of fuel consumption for the current simulation step are defined: in mg/s and L/100 km. In the node evaluation, fuel consumption means the total fuel consumed by one certain vehicle type or all vehicle types in gallons within the selected area. In the network performance evaluation, the fuel consumption reflects the fuel consumed by one certain vehicle type or all vehicle types in kg for the entire network. Also, the fuel consumption can be obtained from the link evaluation, in which it is defined as the fuel consumption during the current interval (mg/m/s).

The fuel consumption model in VISSIM is based on simple calculations taken from the TRANSYT-7F software. This fuel consumption model is a linear function of the total vehicle miles traveled, total signal delay in hours, and total stops in vehicles per hour. The first and third factors are determined based on the average speed of vehicles.

In the case of the INTEGRATION software, second-by-second speed and acceleration data in conjunction with microscopic fuel consumption and emission models are used to estimate a vehicle's instantaneous fuel consumption and emission rate. From a general point of view, the use of instantaneous speed and acceleration data for the estimation of energy and emission impacts of traffic improvement projects provide a major advantage over state-of-practice methods that estimate vehicle fuel consumption and emissions based exclusively on the average speed and number of vehicle miles traveled by vehicles on a given transportation link. These methods assume that differences in driver behavior can be neglected and implicitly assume that all vehicles traveling on a link pollute similarly for an identical average speed and vehicle-miles traveled. In reality, different speed and acceleration profiles with the same average speed and vehicle-miles traveled could result in different levels of fuel consumption and emissions. As with fuel consumption models, the emission models are sensitive to the instantaneous-vehicle speed and acceleration levels. Applications of these models have shown that the emission of compounds, hot-stabilized tail-pipe hydrocarbon (HC), carbon monoxide (CO), carbon dioxide (CO₂), oxides of nitrogen (NO_x), and particulate matter (PM) are related to vehicle travel time, distance, speed, and fuel consumption in an often highly nonlinear fashion. Consequently, traffic management strategies that may have a significant positive impact on one measure are not always guaranteed to have an impact of the same magnitude or even sign on any of the other measures.

The computation of deci-second speeds permits the steady-state fuel consumption rate for each vehicle to be computed each second on the basis of its current instantaneous speed and acceleration level (Rakha, H., et al., 2000; Rakha, H., K. Ahn, and A. Trani, 2003; Rakha, H., K. Ahn, and A. Trani, 2004; Rakha, H. and K. Ahn, 2004; Ahn, K., et al.,

2001; Ahn, K., H. Rakha, and A. Trani, 2004). These fuel consumption and emission models were developed using data that were collected on a chassis dynamometer at the Oak Ridge National Labs (ORNL), data gathered by the Environmental Protection Agency (EPA), and data gathered using an on-board emission measurement device (OBD). The models use instantaneous speed and acceleration levels as independent variables.

As was mentioned earlier the INTEGRATION software incorporates a variable power vehicle dynamics model that computes the vehicle's tractive effort, aerodynamic, rolling, and grade-resistance forces, as described in detail in the literature (Rakha, H., et al., 2001; Rakha, H. and I. Lucic, 2002). The INTEGRATION model has not only been validated against standard traffic flow theory (Rakha, H. and B. Crowther, 2002; Dion, F., H. Rakha, and Y.-S. Kang, 2004; Rakha, H., Y.-S. Kang, and F. Dion, 2001; Rakha, H. and B. Crowther, 2003), but also has been utilized for the evaluation of real-life applications (Rakha, H., 1990; Rakha, H., et al., 2005; Rakha, H., et al., 1998). The types of analyses that can be performed with these built-in models extend far beyond the capabilities of EPA's MOBILE5 model (Rakha, H., K. Ahn, and A. Trani, 2003; Park, S. and H. Rakha, 2006).

In INTEGRATION, the total fuel consumption and average fuel consumption can be obtained from the summary output file. Total fuel consumption on the link (L) is computed as the total volume of fuel consumed by all vehicles traversing the link) from average traffic conditions file (File 11). From time series of traffic conditions file (File 12), total fuel consumption on the link (L) is computed as the total volume of fuel consumed by all vehicles traversing the link. From File 15 and 16 (trip and link level probe statistics), fuel used by vehicle (L) records type differences as per record 10.

Unlike VISSIM, the INTEGRATION software allows the user to override the default vehicle-type-specific fuel consumption factors as well as emission factors, which provides experienced users more flexibility.

4.6 Calibration of steady-state Car-following Model

The modeling and calibration of the INTEGRATION steady-state behavior was described earlier in this paper and thus is not discussed further. In the case of the VISSIM model, the calibration of the model entails calibrating the Wiedemann74 model. In order to calibrate the steady-state Wiedemann74 model the following calibration procedure was developed in an earlier publication (Rakha, H. and Y. Gao., 2008). The calibration of the Wiedemann74 model can be achieved by deriving the speed-flow relationship for the congested regime as

$$q = \frac{1000u}{\frac{1000}{k_j} + \frac{E(BX)E(EX)}{\sqrt{3.6}}\sqrt{u}} \quad (73)$$

Here u is the traffic stream space-mean speed (km/h); q is the traffic stream flow rate (veh/h), and k_j is the traffic stream density (veh/km). By taking the derivative of flow with respect to speed the relationship is demonstrated to be a strict monotonically

increasing function. Consequently, the maximum flow occurs at the boundary of the relationship and thus at the maximum desired or free-flow speed. As was the case with the Pipes' model, the speed-at-capacity equals the free-flow speed. By inputting the maximum flow (capacity) and free-flow speed in Equation (27), removing the $E(EX)$ term to compute the capacity upper bound, and re-arranging the equation; the expected value of BX can be computed as

$$E(BX) = 1000\sqrt{3.6}\sqrt{u_f} \left(\frac{1}{\alpha q_c} - \frac{1}{k_j u_f} \right). \quad (74)$$

By considering that the expected value of SDX is α times the expected value of ABX (i.e. $E(SDX) = \alpha \times E(ABX)$), where the parameter α ranges from 1.5 to 2.5; the expected value of EX can be computed as

$$E(EX) = \frac{\frac{k_j u_f}{\alpha q_c} - 1}{\frac{k_j u_f}{\alpha q_c} - 1} \simeq \alpha \quad (75)$$

Given that $k_j u_f / q_c$ is typically very large, the expected value of EX is approximately equal to the parameter α .

In an attempt to validate the calibration procedure a simple network was coded and simulated using the VISSIM software. The network was composed of two single-lane links in order to isolate the car-following behavior (i.e. remove any possible impact that lane-changing behavior might have on the traffic stream performance). Initially the capacity of both links was set equal using the proposed calibration procedure. The arrival rate was increased gradually until it exceeded the capacity of the entrance link. The traffic stream flow and speed were measured using a number of loop detectors along the first link. The default model randomness was set ($AXadd = 2$, $BXadd = 3$, and $BXmult = 4$). The results demonstrate that the uncongested regime is flat as was suggested earlier, as illustrated in Figure 3-4. Subsequently, the capacity at the downstream link was reduced by selecting the input parameters using the calibration procedures presented earlier. The demand was fixed at the capacity of the upstream link and thus a bottleneck was created at the entrance to link 2. The departure flow rate and speed were directly measured upstream of the bottleneck to construct the congested regime of the fundamental diagram. As demonstrated in Figure 3-4 the simulated data appear to initially follow the ABX curve and then move towards the SDX curve as the capacity of the downstream bottleneck increases. Given that the movement between the two regimes is not documented in the literature it is not clear how this is done. The figure clearly demonstrates that the proposed calibration procedures are consistent with the VISSIM model output.

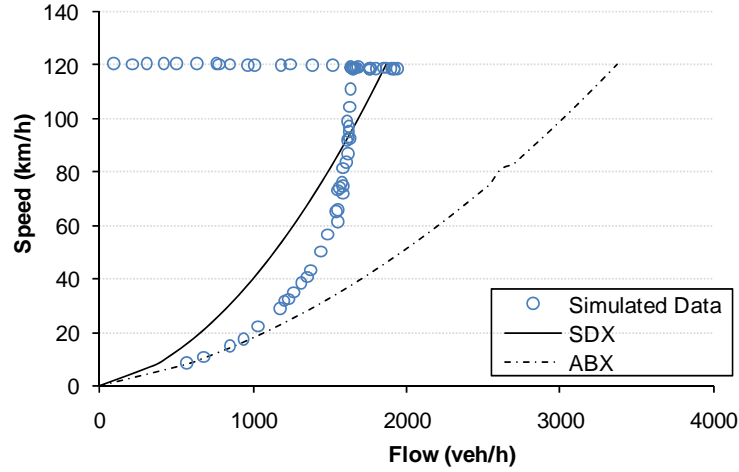


Figure 4-3: Wiedemann74 Calibration Procedure Validation

The VISSIM software also offers a second car-following model, namely the Wiedemann99 model. The model is formulated as

$$u_n(t + \Delta t) = \min \left\{ \begin{array}{l} u_n(t) + 3.6 \cdot \left(CC8 + \frac{CC8 - CC9}{80} u_n(t) \right) \Delta t \\ 3.6 \cdot \frac{s_n(t) - CC0 - L_{n-1}}{u_n(t)} \end{array} , u_f \right\}. \quad (76)$$

This model, as was the case with the Gipps model, computes the vehicle speed as the minimum of two speeds: one based on the vehicle acceleration restrictions and the other based on a steady-state car-following model. The model considers a vehicle kinematics model with a linear speed-acceleration relationship where $CC8$ is the maximum vehicle acceleration at a speed of 0 km/h (m/s^2) and $CC9$ is the maximum vehicle acceleration at a speed of 80 km/h (m/s^2). The VISSIM software also allows the user to input a user-specified vehicle kinematics model that appears to over-ride the linear model. This user specified relationship allows the user to modify the desired and maximum driver speed-acceleration relationship. The second term of Equation (31) computes the vehicle's desired speed using a linear car-following model and thus is identical to the Pipes model.

Consequently, as was done with the Pipes model the model constants $CC0$ and $CC1$ (also known as the Driver Sensitivity Factor) can be computed as

$$CC0 = \frac{1000}{k_j} - \bar{L}, \text{ and} \quad (77)$$

$$CC1 = 3600 \left(\frac{1}{q_c} - \frac{1}{k_j u_f} \right). \quad (78)$$

Where $CC0$ is the spacing between the front bumper of the subject vehicle and the rear bumper of the lead vehicle. This equals the jam density spacing minus the average vehicle length. The Driver Sensitivity Factor ($CC1$) can be calibrated using three macroscopic traffic stream parameters, namely: the expected roadway capacity, jam density, and free-flow speed.

4.7 Comparison of VISSIM and INTEGRATION Results

4.7.1 Network and Modeling Overview

The network used in the study was composed of two 1-km long links. A traffic signal was located at the end of the first link that operated under a fixed-time control with a two phase timing plan, a 50/50 phase split, a cycle length of 60 s, and a yellow time of 5 s per phase. The driver desired speed was set at 100 km/h in the INTEGRATION software by setting a link-specific free-flow speed. Similarly, the desired speed in VISSIM was set by restricting the vehicle's desired speed distribution to range between 99.9 and 100.1 km/h. Only "cars" were simulated in both simulation software applications. Other parameters were kept at default values because most users do not change the default values. However, later these default parameters were modified to demonstrate the impact of these parameters on the model results, as will be discussed later in the paper.

4.7.2 Comparison of Driver Behavior in Response to Traffic Signal Indications

To better illustrate the modeling of driver behavior as they approach the traffic signal, the color of the x-axis is varied to correspond with the traffic signal indication, as illustrated in Figure 4-4. As the vehicle enters the network, the driver faces different signal indications by varying the vehicle entry time from 1 s to 56 s at increments of 5 s.

The comparative results of speed and acceleration profiles are illustrated in Figure 4-. The results demonstrate that the VISSIM model produces small oscillations in the vehicle speed between the minimum and maximum desired speed (99.9 to 100.1 km/h). In all scenarios the vehicle within the VISSIM software reacted to the traffic signal indication at a distance of approximately 167 m upstream of the traffic signal. Figure 4-a and b show that the vehicle in VISSIM reacted later to the signal indication when compared to the INTEGRATION model. Specifically, the INTEGRATION model produces a milder deceleration level of 1 m/s^2 as they approach the red traffic signal. The vehicle acceleration behavior within the INTEGRATION software again demonstrates a more milder buildup and decline in the acceleration level as the vehicle accelerates from a complete stop. When the vehicle enters after 31 s (Figure 4-b) the vehicle within the INTEGRATION software initially decelerates as it approaches the red traffic signal, however the signal indication turns green before the vehicle comes to a complete stop and thus the vehicle accelerates following its initial deceleration maneuver to experience a partial stop.

In the case that the vehicle enters after 41 s both software produce very similar behavior with the vehicle running through the intersection. Alternatively, Figure 4-d demonstrates that when the vehicle enters after 56 s the vehicle within the INTEGRATION software initially attempts to run the yellow light but then has to stop as the traffic light turns red producing an aggressive deceleration maneuver (deceleration level of 7 m/s^2 .)

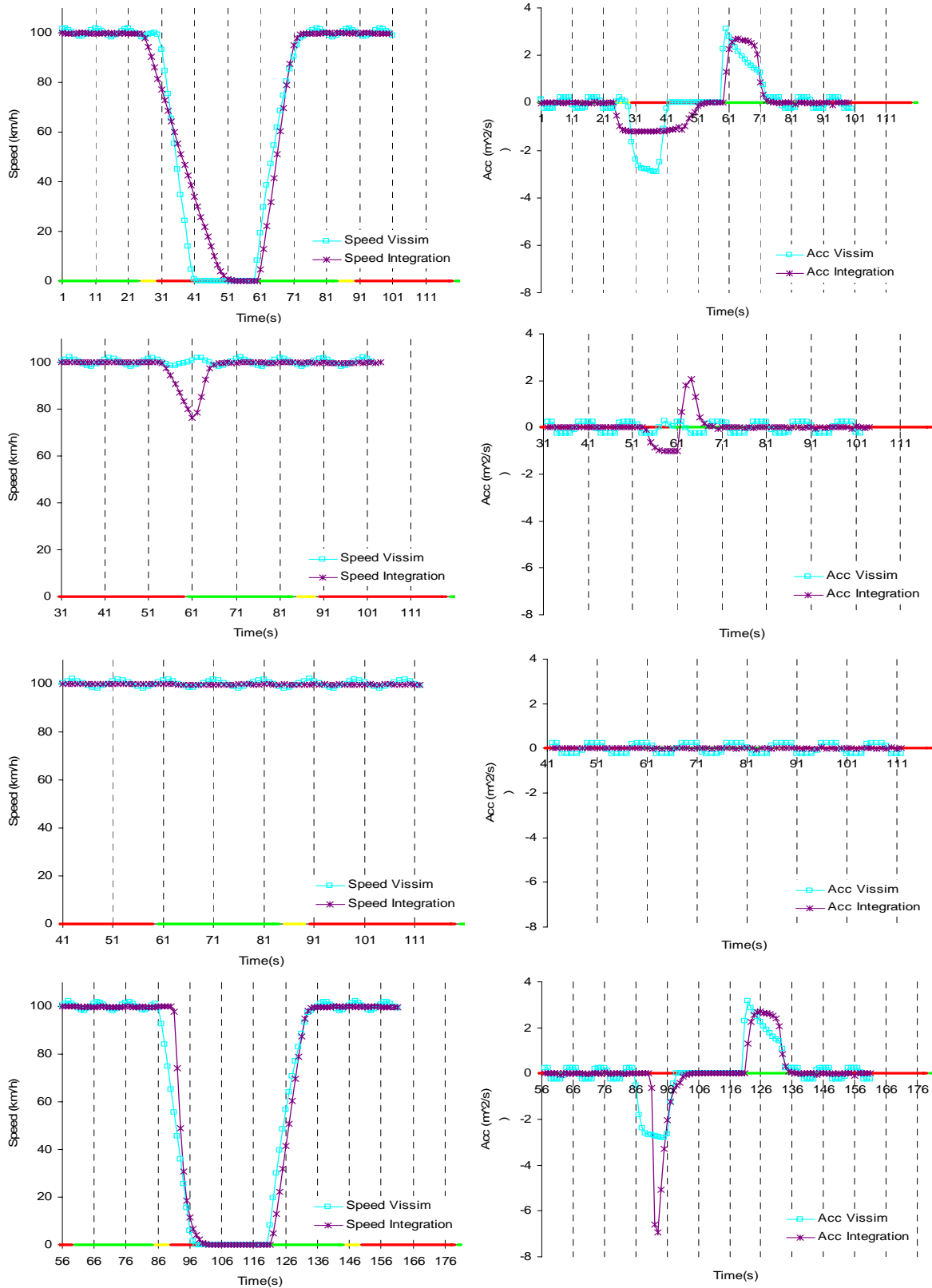


Figure 4-4: Comparison of Vehicle Speed and Acceleration Profiles (a) Entry 1 s; (b) Entry at 31 s; (c) Entry at 41 s; (d) Entry at 56 s

4.7.3 The Effects of the “Look-ahead Distance” on VISSIM Driver Behavior

According to the VISSIM 4.30 User Manual (5), the “look-ahead distance” is the distance that a vehicle can see forward in reacting to other vehicles either in front or to the side of it (within the same link). This section examines the effect of the “look-ahead distance on driver behavior.

The default value for the “look-ahead distance” in VISSIM is a minimum of 0.00 m and a maximum of 250 m. In the previous comparison, the default maximum “look-ahead distance” was 250 m. In this section, a “look ahead-distance” of 150 m to 500 m at 50 m step sizes was considered. Considering a vehicle entry time of 21 s the speed and acceleration profile for different look-ahead distances is illustrated in Figure 4-5.

As seen in the results above, when the “look-ahead distance” was set at 50 m (Figure 4-a), the driver did not have enough time to stop. When the “look-ahead distance” was increased to 90 m, the driver had only a very short distance ahead of the signal to stop, and thus had to stop at an aggressive deceleration level of 6 m/s^2 (Figure 4-c). As the look-ahead distance increased vehicles were able to stop at milder deceleration rates, as demonstrated by the lower deceleration rate at a look-ahead distance of 150 m (Figure 4-d).

Additional runs demonstrated that a 90 m “look-ahead distance” was the boundary condition for reacting to the traffic signal. In this situation, the vehicle used the maximum deceleration rate. When choosing a smaller look-ahead distance, the driver does not have enough time to decelerate and thus runs the red light. Specifically, by selecting a “look-ahead distance” of 89 m, the driver hesitated by decelerating initially and then electing to run the red light, as demonstrated in Figure 4-5-b.

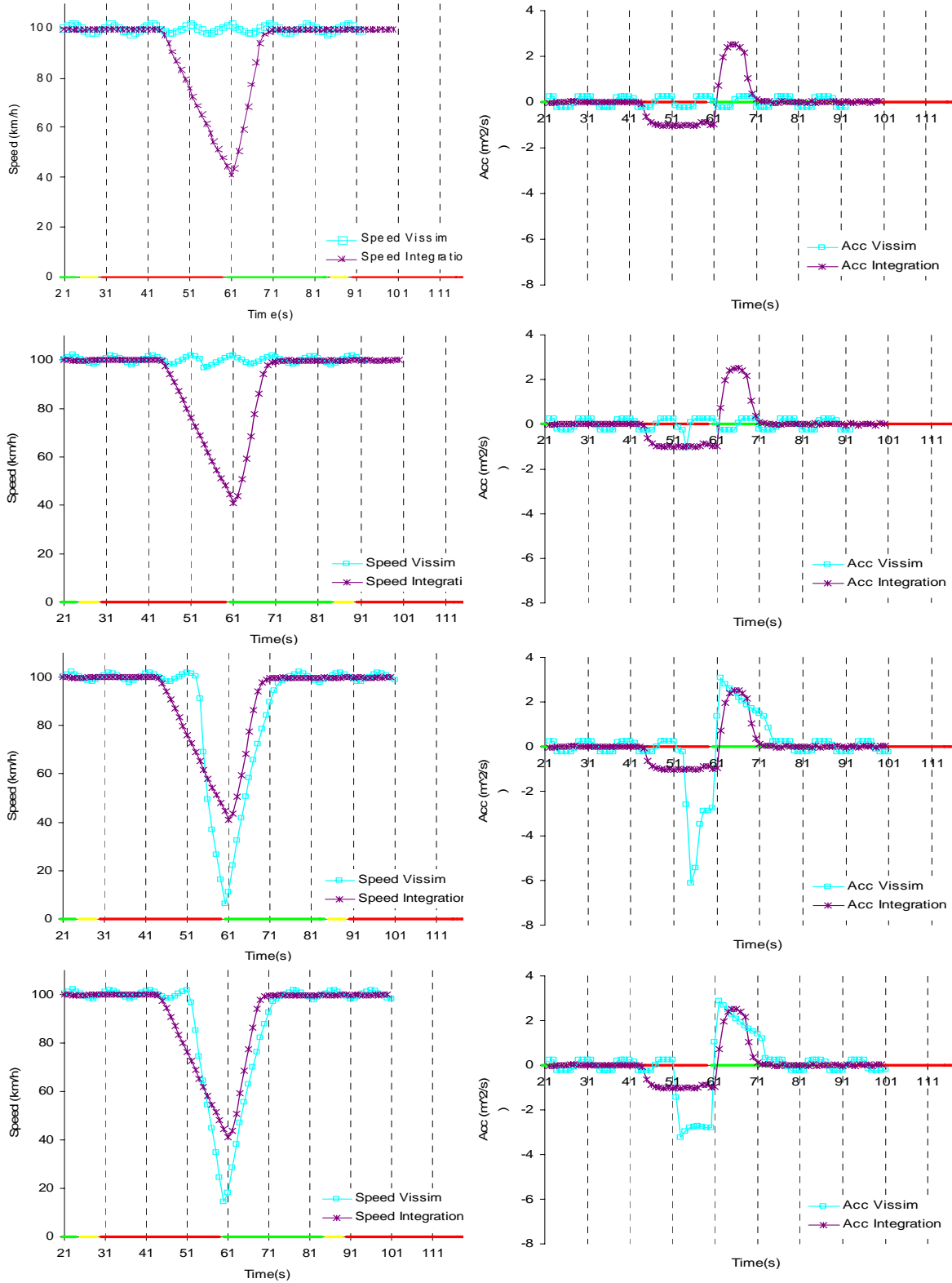


Figure 4-5: Comparison of Vehicle Speed and Acceleration Profiles (a) Look-ahead Distance 50 m; (b) Look-ahead Distance of 89 m; (c) Look-ahead Distance of 90 m; (d) Look-ahead Distance of 150 m

4.7.4 Effect of Braking Ability on VISSIM Driver Behavior

The desired deceleration rate within the VISSIM software was modified and made equal to that used in the INTEGRATION software by modifying the default maximum deceleration level. The default “look-ahead distance” was kept at 250 m and the behavior of the subject vehicle is illustrated in Figure 4-6-a. The figure demonstrates that if the vehicle decelerates at a lower level a look-ahead distance of 250 m is insufficient to make a safe stop and thus the vehicle proceeds to run a red light. When the look-ahead distance is increased to 700 m the vehicle is able to stop, as illustrated in Figure 4-6-b. Consequently, the model user should be very careful in assigning default deceleration and look-ahead distances within the VISSIM software because an alteration of these parameters can result in unrealistic driver behavior.

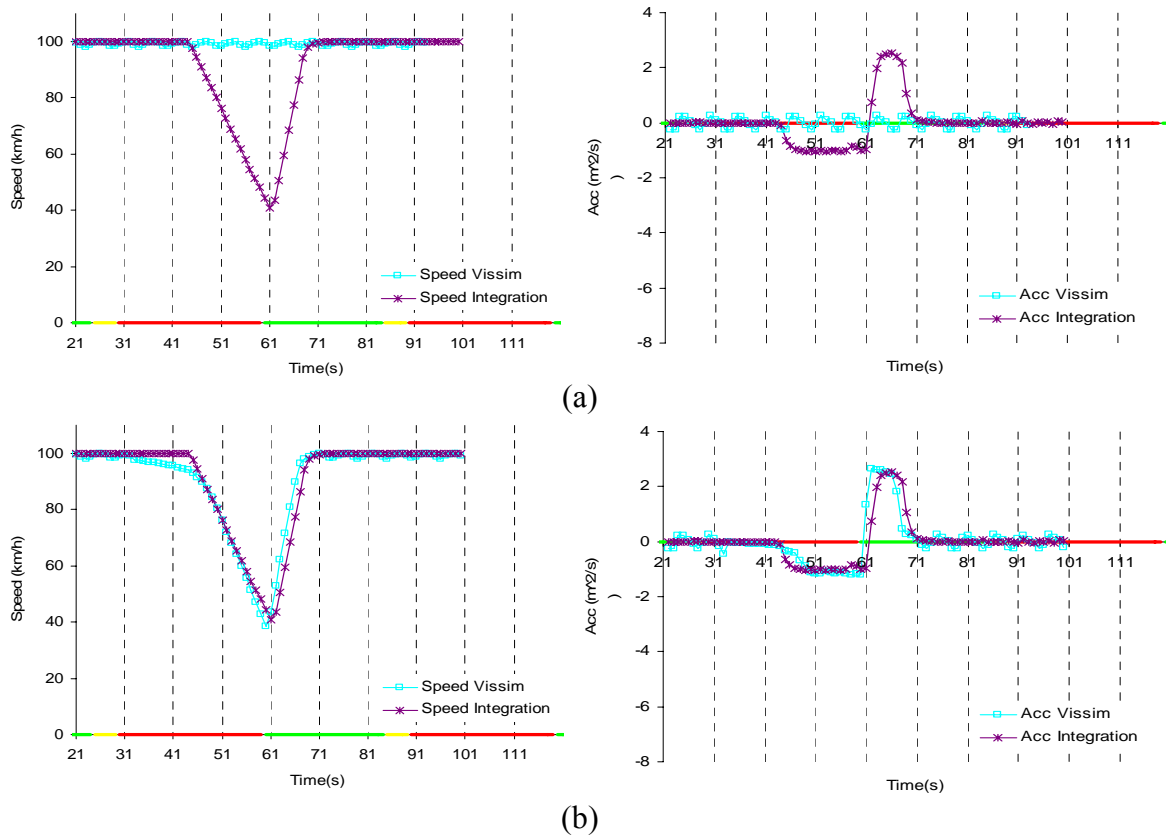


Figure 4-6: Comparison of Vehicle Speed and Acceleration Profiles (a) Look-ahead Distance of 250 m (b) Look-ahead Distance of 700 m

4.7.5 Comparison Driver Behavior Depending on Facility Type

Unlike the INTEGRATION software, the VISSIM model provides the user with two link types: urban and freeway. Figure illustrates a comparison of speed and acceleration profiles for both link types. A key difference in the modeling of different link types is that on urban links the vehicle speed oscillates between the desired minimum and maximum speed. Furthermore, the driver on an urban link appears to react later to a red signal indication and thus decelerates at a higher deceleration.

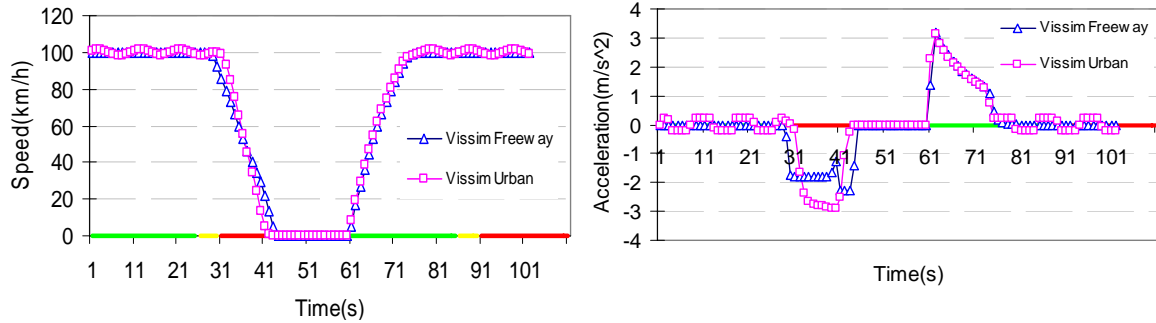


Figure 4-7: Example of VISSIM Urban and Freeway Speed Profile Comparison.

4.7.6 Comparison of Saturation Flow Rates and Discharge Headways

Using the proposed calibration procedures, a base saturation flow rate of 2,304 veh/h was coded for both models. A demand exceeding the capacity of the signalized intersection approach was loaded on the network and the discharge headway at the stop line was recorded. The discharge headway of all vehicles departing during a single cycle length demonstrates that in the case of the INTEGRATION software, the discharge headway decreases and reaches steady-state conditions after approximately 7 vehicles, as illustrated in Figure . In the case of the VISSIM software the variability in the discharge headways appears to be very significant ranging between 0.6 and 2.6 s. The average headway for all vehicles is 1.56 s and 1.68 s in the case of the VISSIM and INTEGRATION software, respectively. These correspond to an average discharge saturation flow rate of 2,308 veh/h and 2,143 veh/h, respectively which corresponds to a 0% and 7% reduction in the saturation flow rate. This reduction in saturation flow rate is consistent with field observations and is attributed the acceleration constraints that are imposed on the car-following model.

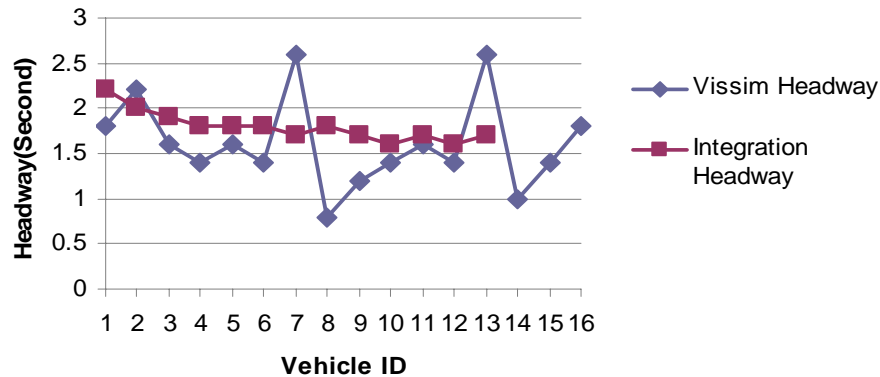


Figure 4-8: Comparison of Discharge Saturation Flow Rates.

The discharge saturation flow rate was also measured downstream the stop line at 100 m increments, as illustrated Figure . The figures show that the discharge rates increase as the traffic stream proceeds downstream. This increase in discharge rate is attributed to the fact that vehicles are able to reach their steady-state as they move forward. Again, this behavior is consistent with field observations.

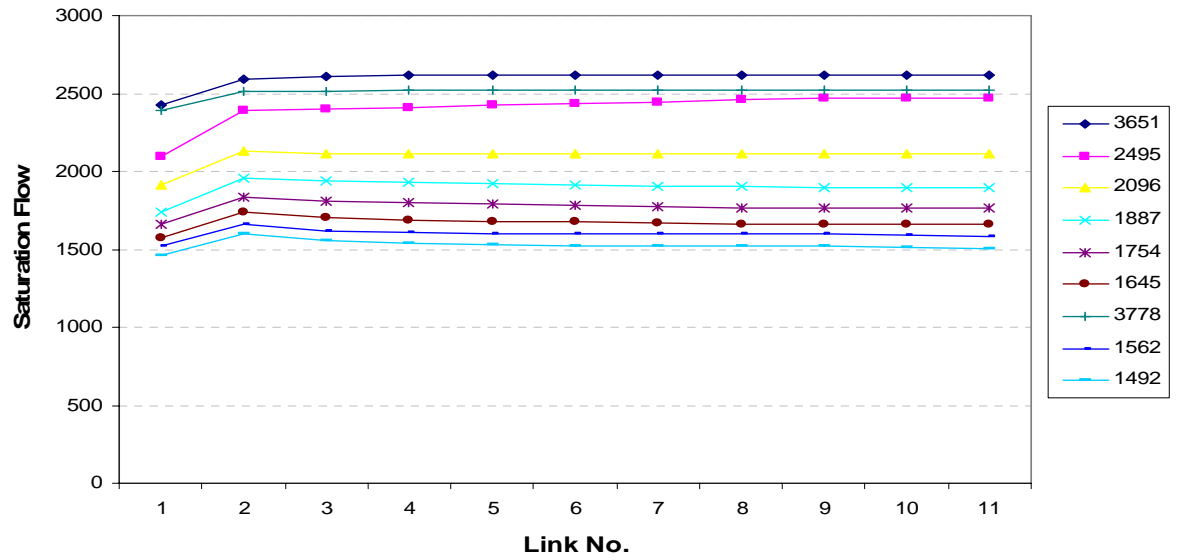
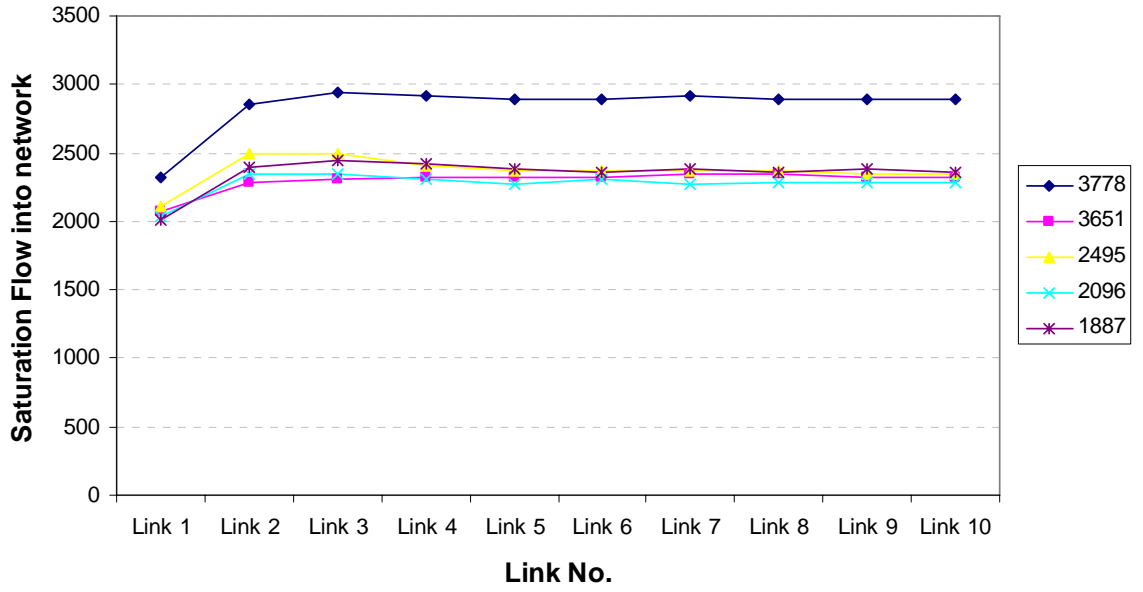


Figure 4-9: Illustration of Discharge Saturation Flow Rates (a) VISSIM and (b) INTEGRATION.

4.7.7 Comparison of Delay Estimates

A comparison of individual vehicle delay estimates as computed by both software demonstrates a high level of consistency, as demonstrated in Figure . Similar results were observed for the total travel time and stopped delay.

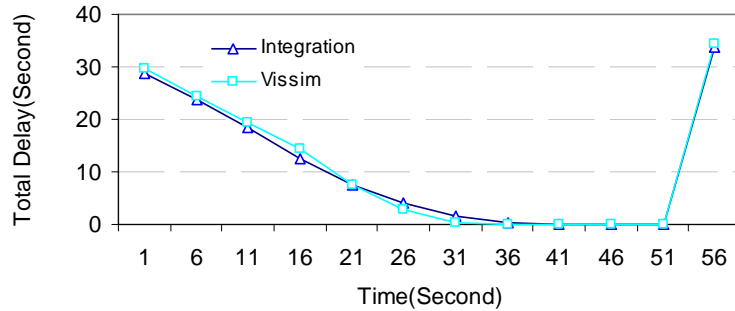


Figure 4-10: Delay Comparison.

4.7.8 Comparison of Fuel Consumption Estimates

The total fuel consumed in the network as computed by the VISSIM and INTEGRATION software was compared. As illustrated in Figure , the fuel consumption in the case of the VISSIM software was lower than that for the INTEGRATION software. Furthermore, given that the VISSIM software uses a more aggregate approach to estimating fuel consumption it is insensitive to transient behavior and thus is fairly flat.

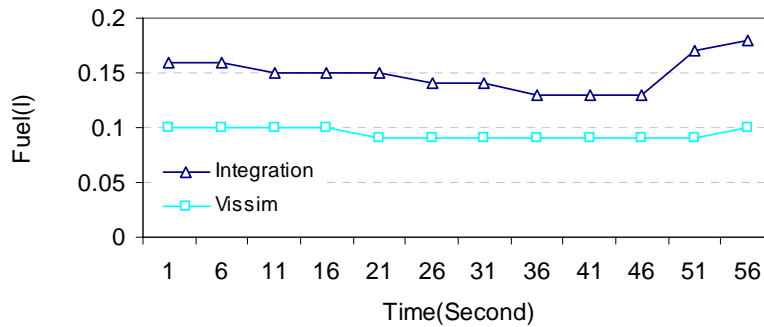


Figure 4-11: Fuel Consumption Comparison.

4.8 Study Conclusions

The paper compares the VISSIM and INTEGRATION software for the modeling of traffic signal networks. The software are compared in terms of the modeling of longitudinal vehicle motion, driver behavior within the traffic signal dilemma zone, vehicle acceleration constraints, vehicle discharge headways, and various measures of effectiveness (delay, stops, and fuel consumption). The results demonstrate that it is possible to calibrate both simulation software using macroscopic loop detector data. Both software incorporate a psycho-physical car-following model which accounts for vehicle acceleration constraints. The INTEGRATION software, however uses a physical vehicle dynamics model while the VISSIM software requires the user to input a vehicle-specific speed-acceleration kinematics model. The use of a vehicle dynamics model has the advantage of allowing the model to account for the impact of roadway grades, pavement surface type, pavement surface condition, and type of vehicle tires on vehicle acceleration behavior. Both models capture a driver’s willingness to run a yellow light if conditions warrant it. The VISSIM software incorporates a statistical stop/go probability model while current development of the INTEGRATION software includes a behavioral model as opposed to a statistical model for modeling driver stop/go decisions. Both software

capture the loss in capacity associated with queue discharge using acceleration constraints. The losses produced by the INTEGRATION model are more consistent with field data (7% reduction in capacity). Both software demonstrate that the capacity loss is recovered as vehicles move downstream of the capacity bottleneck. With regards to fuel consumption and emission estimation the INTEGRATION software, unlike the VISSIM software, incorporates a microscopic model that captures transient vehicle effects on fuel consumption and emission rates.

Chapter 5: Conclusions and Recommendations for Future Study

5.1 Conclusions

The thesis first developed procedures for calibrating the steady-state car-following models utilized in the AIMSUN2, VISSIM, PARAMICS, CORSIM and INTEGRATION software using macroscopic loop detector data and then compared the various steady-state car-following formulations. Through the analysis, it was clear that the Gipps and Van Aerde steady-state car-following models provide the highest level of flexibility and the Van Aerde model, is easier to calibrate given that it is a single-regime model. Subsequently, a detailed comparison of the VISSIM and INTEGRATION traffic simulation models was conducted in order to demonstrate the similarity and differences between these two models. A summary of the two study conclusions are presented in the following sections.

5.1.1 Calibration and Comparison of Steady-state Car-following Models

The study developed procedures for calibrating the steady-state component of various car-following models using macroscopic loop detector data. The paper then compared the various steady-state car-following formulations and demonstrated that the Gipps and Van Aerde steady-state car-following models provide the highest level of flexibility in capturing different driver and roadway characteristics. However, the Van Aerde model, unlike the Gipps model, is a single-regime model and thus is easier to calibrate given that it does not require the segmentation of data into two regimes. An analysis of existing software demonstrated that a number of car-following parameters are network- and not link-specific and thus do not offer model users with the flexibility of coding different roadway capacities for different facility types. In some software, however, arterial and freeway roadway car-following parameters can be coded separately, as in the case of CORSIM and VISSIM. However, major roadway capacity differences can be observed within the broad range of facility categories. For example the saturation flow rate may vary from 1300 to 2000 veh/h on an arterial depending on the roadway and driver characteristics. Consequently, the paper recommends that modifications be made to the various software to allow more flexibility in setting link-specific car-following parameters.

5.1.2 Comparison of VISSIM and INTEGRATION Software

The study compared the VISSIM and INTEGRATION software for the modeling of traffic signal networks. The software were compared in terms of the modeling of longitudinal vehicle motion, driver behavior within the traffic signal dilemma zone, vehicle acceleration constraints, vehicle discharge headways, and various measures of effectiveness (delay, stops, and fuel consumption). The results demonstrated that it is possible to calibrate both simulation software using macroscopic loop detector data. Both software incorporate a psycho-physical car-following model which accounts for vehicle acceleration constraints. The INTEGRATION software, however uses a physical vehicle dynamics model while the VISSIM software requires the user to input a vehicle-specific speed-acceleration kinematics model. The use of a vehicle dynamics model has the

advantage of allowing the model to account for the impact of roadway grades, pavement surface type, pavement surface condition, and type of vehicle tires on vehicle acceleration behavior. Both models capture a driver's willingness to run a yellow light if conditions warrant it. The VISSIM software incorporates a statistical stop/go probability model while current development of the INTEGRATION software includes a behavioral model as opposed to a statistical model for modeling driver stop/go decisions. Both software capture the loss in capacity associated with queue discharge using acceleration constraints. The losses produced by the INTEGRATION model are more consistent with field data (7% reduction in capacity). Both software demonstrate that the capacity loss is recovered as vehicles move downstream of the capacity bottleneck. With regards to fuel consumption and emission estimation the INTEGRATION software, unlike the VISSIM software, incorporates a microscopic model that captures transient vehicle effects on fuel consumption and emission rates.

5.2 Recommendations

As is the case with any research effort, further research is required as follows:

1. Develop calibration procedures for non-steady state car-following behavior.
2. Validate the various car-following models against field data.
3. Develop calibration procedures for other traffic simulation software including the TransModeler, SimTraffic, and MITSIM software.
4. Extend the model comparison by introducing more vehicle types.
5. Conduct a more detailed analysis on vehicle stop computation within VISSIM.
6. Extend the comparison study to include other software.

Bibliography

- Ahn, K., et al., *Estimating vehicle fuel consumption and emissions based on instantaneous speed and acceleration levels*. Journal of Transportation Engineering, 2001. 128(2): p. 182-190.
- Ahn, K., H. Rakha, and A. Trani, *Microframework for modeling of high-emitting vehicles*. Transportation Research Record. , 2004(1880): p. 39-49.
- Brackstone, M. and M. McDonald, *Car-following: a historical review*. Transportation Research, 1999. 2F: p. 181-196.
- Barcelo.J. et al (2004), “ Microscopic traffic simulation: A tool for the design, analysis and evaluation of intelligent transport systems” Journal of Intelligent and Robotic Systems, Volume 41, Numbers 2-3, January 2005 , pp. 173-203(31)
- Demarchi, S.H. *A new formulation for Van Aerde's speed-flow-density relationship. (in portuguese)*. in XVI Congresso De Pesquisa e Ensino em Transportes. 2002. Natal, RN, Brazil.
- Dowling, R., et al., *Guideline for Calibration of Micro-simulation Models: Framework and Applications*. Transportation Research Record, 2004. 1876: p. 1-9.
- Dion, F., H. Rakha, and Y.-S. Kang, *Comparison of delay estimates at under-saturated and over-saturated pre-timed signalized intersections*. Transportation Research Part B Methodological, 2004. 38(2): p. 99-122.
- Farzaneh, M. and H. Rakha, *Impact of differences in driver desired speed on steady-state traffic stream behavior*. Transportation Research Record: Journal of the Transportation Research Board, 2006. 1965: p. 142-151.
- Fritzsche, H-T. (1994). “A model for traffic simulation” Transportation Engineering Contribution 5: 317-321
- G.Duncan (2000), Paramics Technical Report:Car-Following, Lane-Changing and Junction Modelling
- Gazis, D., R. Herman, and R. Rothery, *Nonlinear follow-the-lead models of traffic flow*. Operations Research, 1961. 9(4): p. 545-567.
- Gipps, P.G., *A behavioral car-following model for computer simulation*. Transportation Research, 1981. 15B: p. 105-111.
- Halati, A., H. Lieu, and S. Walker, *CORSIM- Corridor Traffic Simulation Model in 76th Transportation Research Board Meeting*. 1997: Washington DC.
- T. Jiménez et al (2004), “A road traffic simulator: Car-following and lane-changing”

Proceedings of the 14th European Simulation Multiconference on Simulation and Modelling: Enablers for a Better Quality of Life, pp 241-245

Kan. S and Bhan. G (2007) "Evaluation of microscopic lane change models using NGSIM data" Proceedings of the 18th conference on Proceedings of the 18th IASTED International Conference: modeling and simulation. pp: 592 - 597

Loren Bloomberg and Jim Dale (2000) "A Comparison of the VISSIM and CORSIM Traffic Simulation Models on a Congested Network"

M. F. Aycin and R. F. Benekohal (1999), "Comparison of Car-Following Models for Simulation". Transportation Research Record, No.1678, pp.116-127

Moen et al.(2000), A Comparison of the VISSIM Model to Other Widely Used Traffic Simulation and Analysis Programs, Institute of Transportation Engineers

Mannering, F.L. and W.P. Kilareski, *Principles of Highway Engineering and Traffic Analysis*. Second ed. 1998: John Wiley & Sons.

Minnesota Department of Transportation,(2004), Advanced CORSIM Training Manual

Olstam, J. and A. Tapini, *Comparison of Car-Following Models*, in *VTI Publication M960A*. 2004, Swedish National Road and Transport Research Institute: Linköping, Sweden.

Ozaki, H., *Reaction and Anticipation in the Car-following Behavior*, in *12th International Symposium on Transportation and Traffic Theory*. 1993, Elsevier. p. 349-366.

Panwai, S and Dia, H, (2005), "Comparative evaluation of microscopic car-following behavior" IEEE Transactions on Intelligent Transportation Systems, Vol. 6, No. 3,

P. G. Gipps.(1986) "A model for the structure of lane-changing decisions." Transportation Research B, 20B(5):403-414,

PTV, *VISSIM 4.30 User Manual*. 2007: Portland, Oregon.

Prevedouros, P.D., W. James, and J. Jerry. *Tests of simulation models FREQ, KRONOS, INTEGRATION and VISSIM in replicating congested freeway flow*. in *Applications of Advanced Technology in Transportation - Proceedings of the Ninth International Conference on Applications of Advanced Technology in Transportation*. 2006. Chicago, IL, United States: American Society of Civil Engineers.

Park, S. and H. Rakha, *Energy and Environmental Impacts of Roadway Grades*. Transportation Research Record, 2006. 1987: p. 148-160.

Quadstone (2003): Quadstone PARAMICS Version 4.1, User Guides, Edinburgh, Scotland

Rakha H. and Crowther B. (2003), "Comparison and Calibration of FRESIM and INTEGRATION Steady-state Car-following Behavior", *Transportation Research* , 37A, pp. 127

Rakha H. and Crowther B. (2002), Comparison of Greenshields, Pipes, and Van Aerde Car following and Traffic Stream Models, *Transportation Research Record* , No. 1802, pp. 248-262

Rakha H. and Zhang Y. (2004), The INTEGRATION 2.30 Framework for Modeling Lane-Changing Behavior in Weaving Sections, *Transportation Research Record: Journal of the Transportation Research Board*, No. 1883, pp. 140-149

Rakha, H., P. Pasumarthy, and S. Adjerid. *The INTEGRATION framework for modeling longitudinal vehicle motion*. in *TRANSTEC*. 2004. Athens, Greece.

Rakha, H.A. *Validation of Van Aerde's simplified steady-state car-following and traffic stream model*. in *85th Transportation Research Board Annual Meeting*. 2006. Washington D.C.: Transportation Research Board.

Rakha, H., C.C. Pecker, and H.B.B. Cybis. *Calibration procedure for the Gipps' car-following model*. in *86th Transportation Research Board Annual Meeting*. 2007. Washington, DC: Transportation Research Board.

Rakha, H. and M. Arafteh. *Tool for calibrating steady-state traffic stream and car-following models*. in *Transportation Research Board Annual Meeting*. 2007. Washington, D.C.: TRB.

Rakha, H., et al., *Vehicle dynamics model for predicting maximum truck acceleration levels*. *Journal of Transportation Engineering*, 2001. 127(5): p. 418-425.

Rakha, H. and I. Lucic, *Variable power vehicle dynamics model for estimating maximum truck acceleration levels*. *Journal of Transportation Engineering*, 2002. 128(5): p. 412-419

Rakha, H., M. Snare, and F. Dion, *Vehicle dynamics model for estimating maximum light-duty vehicle acceleration levels*. *Transportation Research Record*, 2004. n 1883: pp. 40-49.

Rakha, H., Y.-S. Kang, and F. Dion, *Estimating vehicle stops at undersaturated and oversaturated fixed-time signalized intersections*. *Transportation Research Record*, 2001. n 1776: p. 128-137

Rakha, H., et al., *Requirements for evaluating traffic signal control impacts on energy and emissions based on instantaneous speed and acceleration measurements*. *Transportation Research Record*, 2000. n 1738: p. 56-67

Rakha, H., K. Ahn, and A. Trani, *Microscopic modeling of vehicle start emissions*. *Transportation Research Record* , 2003(1842): p. 29-38

Rakha, H., K. Ahn, and A. Trani, *Development of VT-Micro model for estimating hot stabilized light duty vehicle and truck emissions*. *Transportation Research*, Part D:

Transport & Environment, 2004. 9(1): p. 49-74.

Rakha, H. and K. Ahn, *Integration modeling framework for estimating mobile source emissions*. Journal of Transportation Engineering, 2004. 130(2): p. 183-193.

Rakha, H., *An Evaluation of the Benefits of User and System Optimised Route Guidance Strategies*, in *Civil Engineering*. 1990, Queen's University: Kingston. p. 168.

Rakha, H., et al., *Evaluating alternative truck management strategies along interstate 81*. Transportation Research Record, 2005. n 1925: p. 76-86.

Rakha, H., et al., *Construction and calibration of a large-scale microsimulation model of the Salt Lake area*. Transportation Research Record, 1998. n 1644: p. 93-102.

Rakha, H. and Y. Gao. *Calibration of Steady-state Car-following Models using Macroscopic Loop Detector Data*. in *Symposium on The Fundamental Diagram: 75 Years*. 2008. Woods Hole, MA.

Skabardonis A. (1999). *Assessment of Traffic Simulation Models*, University of California, Berkley, Institute of Transportation Studies.

TSS-Transport Simulation System (2002), GETRAM/AIMSUN version 4.1 User's Manuals

TSS-Transport Simulation System (2006) AIMSUN 5.1 Microsimulator User's Manual

U. Sparmann(1978), *Spurwechselforgänge auf zweispurigen BAB-Richtungsfahrbahnen*, Forschung Straenbau. und Straenverkehrstechnik, Heft 263

Van Aerde, M. (1995). "Single regime speed-flow-density relationship for congested and uncongested highways." Presented at the 74th TRB Annual Conference (Paper No. 95080), Washington, D.C.

Van Aerde, M. and H. Rakha, *INTEGRATION © Release 2.30 for Windows: User's Guide Volume I: Fundamental Model Features*. 2007, M. Van Aerde & Assoc., Ltd.: Blacksburg.

Van Aerde, M. and H. Rakha, *INTEGRATION © Release 2.30 for Windows: User's Guide – Volume II: Advanced Model Features*. 2007, M. Van Aerde & Assoc., Ltd.: Blacksburg.

Van Aerde, M. and Rakha, H. (1995). *Multivariate calibration of single regime speed-flow density relationships*. Proceedings of the Vehicle Navigation and Information Systems (VNIS) Conference, Seattle, WA, August.

Wiedemann, R.(1974)., *Simulation des straßenverkehrsflusses*, in *Shriftenreihe des Instituts für Verkehrswesen der Universität Karlsruhe, Heft 8*. Universität Karlsruhe.

Wilson, R.E.,(2001) *An analysis of Gipps' car-following model of highway traffic*. IMA Journal of

Applied Mathematics. 66: p. 509-537.

Xiao et al,(2005), "Methodology for Selecting Microscopic Simulators: Comparative Evaluation of AIMSUN and VISSIM", University of Minnesota, Center for Transportation Studies.